CR-184178

Space Transfer Concepts and Analysis for Exploration Missions

Contract NAS8-37857

Final Report
Task Directive 5
March 1991

Boeing Defense & Space Group
Advanced Civil Space Systems
Huntsville, Alabama

D615-10031-1

Abstract

The current study is the second phase of a broad-scoped and systematic study of space transfer concepts for human Lunar and Mars missions. The one month Technical Directive 5 is a short follow-on to the initial contract. During this period, relevant space transportation studies were initiated to lead to further detailed activities in the following study period.

Key Words

Architecture
Habitats
Life Cycle Cost
Manifesting
Missions (Lunar and Mars)
Space Propulsion
Space Vehicle Concepts
Trajectories

TABLE OF CONTENTS

APPENDICES

1. INTRODUCTION

The first phase of the technical work carried out in the "Space Transfer Concepts and Analysis for Exploration Missions" contract performed by Boeing Aerospace and Engineering under Contract NAS 8-37857 was completed January 1991. In the month of February, Technical Directive 5 was provided to BA&E for additional tasks relating to space exploration studies. The activities conducted during this short duration Technical Directive are described in the text that follows. This initial work is a prelude for the work to follow on the remaining portion of the contract.

The tasks addressed include:

- Vehicle Integration
- Aerobrake Integration Analysis
- Assembly Operations and ETO Vehicle Size Requirements
- Transportation Crew Module and Habitat Update
- Radiation Analysis
- Flight Dynamics Support
- Architecture Assessment, Programmatic Analysis and
  Technology Advancement Priorities and Recommendations
- Support to MSFC SEI Activities

2. VEHICLE INTEGRATION

2.1 Introduction

The Space Transfer Concepts and Analysis for Exploration Missions (STCAEM) Phase 1 study identified the Nuclear Thermal Rocket (NTR) as the most versatile high-performance candidate for Mars missions for reasonable SEI program scales. The STCAEM Phase 2 Vehicle Integration task, begun in Technical Directive 5 (TD5), is investigating the integration issues of the NTR propulsion system in sufficient detail to determine system operations protocols, determine subsystem mass with greater fidelity, identify areas requiring focused technology development, and develop specific requirements for vehicle assembly, processing, inspection, verification, use and refurbishment.

Specifically, Phase 2 has targeted four areas of work in detailing the NTR propulsion subsystem:

a. Discussion of issues, options, selections and rationales for the NTR propulsion subsystem.

b. Schematics and definition of interfaces for the engine/reactor, tanks, propellant feed lines, pressurization subsystem, and power/data/control lines.

c. Sizing of fluid lines and electrical lines.

d. Implications for vehicle test, pre-flight operations (LEO integration), and in-flight operations.

TD5 has accomplished the initial portions of work in the first three areas listed. Most effort has focused on formulating the investigation strategy, developing the calculation methodologies, and exercising bounded-problem cases pertinent to the NTR design. The propulsion subsystem involves a complex set of interrelated design issues, and the TD5 effort represents the initial "tip" of that large iceberg. A summary of the NTR propulsion system definition accomplished so far is followed by technical backup material on line sizing, the design of the pressurization subsystem, and schematics.

2.2 Subsystem Overview

Solid-core nuclear rocket propellant feed systems are essentially the same as for the H2 portion of a LH2/LO2 chemical engine. The propellant flowing from the pump enters the nozzle, flows upward through the neutron reflector surrounding the reactor core, cooling both the reflector and the control drums contained within it, and through a neutron and gamma ray shield placed at the upper end of the reactor assembly to limit the radiation-heating of propellant in the tank. The propellant flows downward through the reactor fuel element cooling passages, reaching the nozzle inlet design temperature before exiting the nozzle plenum chamber prior to being discharged through the exhaust nozzle. A portion of the propellant flow is bled off from this chamber and cooled to an acceptable inlet temperature for the pump drive turbine. This cooling is accomplished primarily by mixing the heated material with cold fluids. A small amount of gas is also drawn from the turbopump outlet for pressurization of the propellant tanks.

The propellant feed system consists of one or more turbopumps, a propellant source, and a system of pipes and valves, including control valves. These components differ from similar components found in liquid chemical rockets only in the modifications required to allow them to survive and function properly in the reactor radiation environment. Of typical and primary concern in this respect are valve seats, seals, bearing lubricants, and rolling contact bearing retainers. In cryogenic chemical rockets, these are usually made of organic materials that are subject to severe damage under neutron and gamma bombardment. Also, valve actuators in most chemical rocket systems are of the hydraulic type and the fluids involved would change in a nuclear rocket either becoming highly viscous or evolving gases under the action of high-energy radiation. Consequently, pneumatically- or electrically-operated devices must be used in the nuclear rocket engines. Radiation heating, though it must be considered in the design, does not pose a significant problem in most of the components of this system due to the high flow rates of cryogenic hydrogen in contact with the components.

The principal subassembly of the propellant feed system is the turbopump and the primary factors influencing the design of this unit are reliability, efficiency, and weight. Pump efficiency is affected not only by the particular design selected, but also by the net positive suction head (NPSH); i.e., the difference (available at the pump inlet) between the total absolute pressure and the fluid vapor pressure. This effect is particularly apparent if the NPSH is low.

An important factor in pump selection involves the characteristics of the start transient. Unless the pump is rechilled, large thermal gradients will exist in the assembly when the propellant valve is first opened, and two-phase flow will occur in the system. This condition will result in some oscillation or pulsation in the flow and may cause engine-start problems.

2.3 Propellant Feed System /Major Elements Description

The Mars Transfer Vehicle (MTV) umbilicals carry fluids, gases, signals and electrical power between the tanks and the engine. During engine thrusting, H2 propellant, under an internal tank pressure, flows to the engine through a series of propellant lines. The propellant passes through a system of manifolds, distribution lines and valves to the engine. The valves are under direct control of the vehicle flight control system computers and are electrically actuated. H2 pressurant gases tapped from the engine are routed back to the tanks through the gas pressurant lines in order to maintain pressure in the tanks.

a. Tanks - At the forward end of each H2 propellant tank is a vent and relief valve. This valve is a dual function valve: it can be opened by helium (vent) or excessive tank pressure (relief). This vent is available only in prelaunch; once lift-off has occurred, only the relief function is operable. The LH2 tanks will relieve at an ullage pressure of 15 psig. Normal tank ullage pressure range during the mission for the LH2 tanks is 10 to 14.7 psia.

In addition to the vent and relief valves the LH2 tanks have a special purpose vent valve that is opened during the tank jettison sequence. A thrust force provided by opening the valve imparts a velocity to the tank to assist in the separation maneuver.

Each H2 tank has four propellant disconnects: two for the LH2 propellant lines (one main and one redundant) and two for the gaseous H2 pressurant lines (main and redundant). Major elements included in the tankage system are the following:

(1) GH2 pressuration lines
(2) LH2 line and tank-vehicle quick disconnect valves
(3) Fuel depletion sensors
(4) Liquid acquisition devices

(5) Anti vortex baffle near liquid acquisition device
(6) Pressure and temperature sensors
(7) Tank loading sensors LH2 ullage pressure sensors
(8) Special purpose valves
(9) MLI and vapor cooled shields
(10) Meteor debris shield

b. Helium Tank Pressurant System (transient) - Initial (start transient) tank pressurization is provided by the high pressure helium gas system. Helium gas at 3000-5000 psia is stored in titanium liner/composite overwrap high pressure tanks. When needed for tank pressurization, the gaseous helium passes through the pressure regulation, valveing, and distribution line systems to the H2 tanks to provide tank pressurization until H2 gas from the engine can be tapped from the turbopumps and routed to the tanks through the H2 gas pressurant line system.

c. Gaseous H2 Tank Pressurant System (steady state) - Internal pressure in the H2 tanks is maintained by the gaseous H2 for the duration of the propulsive burn.

d. Propellant Line, Valve and Turbopump Cooldown - Approximately 1 hr before engine start, LH2 propellant is released into and through the propellant delivery system. This propellant chills down all the LH2 lines, manifolds and valves between the tank and the engine turbopumps so that the path is free of GH2 bubbles and is at the proper temperature for engine start.

e. Post Burn Propellant Tank Jettison - The interface between the individual tank LH2 propellant lines and the vehicle LH2 manifold is a self-sealing quick disconnect. The interface between the tank GH2 pressurant line and the GH2 manifold is also a self-sealing quick disconnect. The tank separation maneuver is preceded by valve closure to isolate the empty tank from the rest of the propellant line system. The tank release mechanism is then activated, and the tanks are pushed away from the vehicle mechanically. The special purpose vent valves supplement the separation release mechanism with a small thrust force driven by tank internal pressure.

f. Tank Attachment and Disconnect - Tank disconnect occurs on the tank side of the LH2 line manifold. Self sealing liquid and gas quick disconnects are provided to allow the complete tankage system to be jettisoned after a propulsive burn and also to allow the reattachment of a new fully loaded tankage system in Earth orbit for reuse on another mission. In addition to the liquid propellant and gaseous pressurant disconnects, power and data cable disconnects are also provided for.

g. System Verification Tests - It is desirable to have the capability to conduct a complete checkout test verifying the tankage system and all its subsystems fully loaded on the launch vehicle while on the pad before launch. After launch and attachment to the orbiting NTR vehicle, LH2 propellant is transfered to the tank to top off the LH2 level in the tank. A complete tankage system and propellant flow test is also conducted after vehicle assembly in orbit for identification and possible replacement of suspect subsystems.

2.4 Propulsion System Schematics

Some schematic diagrams for the hydrogen propellent flow, three turbopump engine configuration, hydrogen and helium gas pressurant flow and hydrogen tank are illustrated in Figures 2-1 to 2-4.

2.5 Fluid Lines

Different sections of the piping would be exposed to different combinations of cryogenic temperature, nuclear radiation, and chemical attack by hydrogen. Materials most suitable for piping are special alloys of aluminum, titanium, and stainless steel. Stainless steel was chosen for application as the H2 propellant line and the gaseous H2 pressurant lines.

The fact that hydrogen can be used for auxiliary as well as for primary needs implies that two systems of piping are required. The primary piping is concerned with large flow rates, intermittent flow, and phase transition from LH2 to GH2. The secondary piping is concerned with low flow rates, continuous flow, and all GH2. These features are summarized in the Figure 2-5.

2.6 Supporting Data

2.6.1 Propellant Line Size Determination Procedure

The procedure to determine the propellant line size is indicated below.

a. Friction loss factors were determined for the assumed piping configurations.

b. Reynolds number for given flow rate, and ε/d value for stainless steel pipe used to determine friction factor (f) from Moody diagram.

c. Friction loss factor for pipe flow determined ($k=fL/d$).

d. Overall line pressure drop calculated for the system ($P_{drop}=(\Sigma k)\rho V^2/2$).

e. Pressure drops plotted vs. line diameter to identify a reasonable point of diminishing returns for increased line diameters.

f. Other factors affecting line size determination system operating parameters, required turbopump inducer inlet conditions, and the worst case degree of LH2 subcool at the tank outlet.

g. STS line sizing example served as a test case for the proposed procedure, although turbopump inlet fluid conditions were different (higher acceleration head available than NTP system).

Sample calculations relating to the propellant line size and pressure drop are provided in Figures 2-6 to 2-11.

2.6.2 Tank Pressurization System Analysis

The assumptions employed in the analysis are given below.

a. Conservation Net Positive Suction Head (NPSH) value of zero assumed for analysis, based on Rocketdyne test results with MK-25 NERVA unit. More advanced pumps with lower NPSH requirements (i.e. negative) may be available for a future NTP system.

b. Degree of subcool attained for H2 by pressurizing storage tanks to approximately 6-8 psi.(41-55kPa) above their normal operating pressure (101.3kPa/15 psia). For example, 15 psi to 22 psi increase in tank pressure results in ~13kJ/kg subcool in the LH2. This degree of subcool must be below the energy added to the fluid by environmental and pressurant gas heating, and propellant delivery line losses.

c. Environmental heating determined from CRYSTORE boiloff code. Preliminary analysis results show that aft tank radiation heating effects are small in comparison to environmental heating (Radiation heating<5% of environmental heating during burn time, assuming all neutrons adsorbed at an average energy level of 2.5 MeV).

d. Pressurant gas heating assumed to consist mainly of free convection (during burn only), and gas conduction.

e. Delivery system propellant heating determined from environmental heating (while in delivery system), and line losses. This heating not a large driver in the level of subcool loss. Line pressure losses, and therefore line sizes, can be determined based on tank pressures and NPSH requirements.

f. Pressurant gas requirements too high for helium pressurization. Helium utilized for initial tank pressurization, line chilldown, and engine start-up (first 30 seconds of burn). Hydrogen bleed from turbopump utilized for steady-state operation.

g. Propellant heating after initial over-pressurization mainly due to free and forced convection at the liquid surface from the pressurant gas (helium and hydrogen). Forced convection considered small if suitable diffuser used for pressurant gas inlet.

h. Free convection heat transfer is the largest single contributor to the subcooled propellant, but it only occurs during burn periods (~ 1 hour for TMI).

(1) A preliminary assessment of allowable heat leak allowed in order for the fluid to remain subcooled for the entire duration of the 3 TMI burns (completed over approx. 24 hours).

(2) Results showed that the cumulative heating on the TMI propellant would remain below allowable limits if the high temperature turbine bleed gas is both throttled (to reduce pressure), and cooled by the pump exit fluid flow below ~100 K before being injected into the tank.

(3) The effects of helium "blanketing" of the fluid were not considered so the allowable inlet gas temperature may be higher.

i. The initial pressurization system (helium) can be one of two major types:

(1) Internal storage systems require smaller tank sizes, due to the higher He gas density at 20 K, versus about 180-200 K for external systems. Composite tanks may not be applicable for this low temperature. The higher storage density is somewhat offset by the higher density of the helium in the ullage.

(2). External storage systems require higher tankage mass, and also require significantly less gas for ullage pressurization. Significant amounts of heat are transferred to the LH2 from the warmer (180-200 K) helium.

j. Helium system mass estimates:

(1) External System - He~~44 kg.
Tanks~~250 kg.
Total=~294 kg. (per TMI tank)

Note: High temperature gas can reduce subcool level by as much as 0.7 kJ/kg. (~5%).

(2) Internal System - He~~160 kg.
Tanks~~220 kg.
Total=~380 kg. (per TMI tank)

k. Propellant line chilldown fluid requirements:

(1) Line Diameter - 10" (25.4 cm.); Length - 70 m.; thickness - 0.4 mm. H2 mass vaporized to bring fluid lines down to 20 K ~ 225 kg. (This vaporized fluid can be expanded through the engine to provide a measure of thrust).

2.6.3 Allowable Line Pressure Drop Results

Some results based upon the allowable line pressure drop are given. (See Figure 2.12)

a. Pressure drop curves utilized to identify acceptable range of line sizes (at "knee" of curve or below).

b. Minimum overpressurization determined to provide adequate liquid subcool is determined (~22 psia).

c. Smallest allowable line size selected to satisfy pressure drop and energy addition requirements.

(1) Maximum pressure drop: 22 psi - 14.696 psi (operating pressure)=~7 psia.

$$NPSH=Pi/\rho+v^2/(2g)-Hvp+Hc$$

NPSH - Net positive suction head required by pump (assumed = o Pa).

Pi - Inlet suction pressure (pressure at storage tank outlet).

ρ - Density of fluid (~70.6 kg./m^3).

v - fluid velocity (m/s). g - Acceleration level (m/s^2).

Hvp - Vapor pressure of luid at pump inlet (~126700 Pa).

Hc - Pressure head between Pi and cneter line of turbopump (Pa.)

Equal to acceleration head - pressure drop in lines.

Maximum pressure drop allowable in tank and delivery propellant lines for 22 psi tank ~3.76 psi* (25.89 kPa).

(To provide ~21K saturated liquid H2 at TP inlet)

* Corresponds to 8" tank line diameter, and 11-12" main delivery line diameter. Line sizes may be small if valves, bends, etc. minimized.

2.6.4 Boiloff Loss Estimate for Dropping Multi-Use Tank Pressure

Pdrop = 22 psia.-14.7 psia = 7.3 psia (50.3 kPa)

Fluid is assumed to reach saturation conditions at the elevated pressure (22 psia/150 kPa)

a. TMI Tanks

After first burn (2/3 full):		After second burn (1/3 fill):	
Fluid loss ≈ 1655 kg.		Fluid loss ≈ 828 kg.	
Vapor loss ≈ 151 kg.		Vapor loss ≈ 302 kg.	
Total	1806 kg.	Total:	1130 kg.

Grand Total ≈ 2936 kg. (~1.3 % of initial load)

The fluid losses can be reduced by designing a thermal protection system, and tank pressurization system that reduces the parasitic heat leak to a minimum, during engine burn.

2.6.5 Summary and Conclusion

a. Turbopump selection will likely drive both pressurization and delivery system design. The main focus of this study was deriving a satisfactory procedure for system design, given pump inlet fluid condition requirements.

b. Process can be automated by assembling the major elements into a computer code. Improved tank pressurization/heating codes will improve confidence significantly.

c. Assumptions of propellant line bends, branch lines, valves, etc. resulted in uncertainty in overall pressure drop calculations. Therefore, pressure drops resulting in Pi values in the range of 22 to 26 psi considered reasonable.

d. Pressurization system selection:

(1) Initial and start-up pressurization - Helium system selected due to its simplicity and reasonable low overall system mass (~0.4% of propellant mass). Internal and external systems are close enough in mass to facilitate the decision to be made based on operational and safety considerations.

(2) Remaining pressurization, after start-up, provided by H2 bleed from turbopumps, because of the prohibitive mass penalty associated with helium use (>10mt/tank).

e. Allowable temperature for turbine bleed inlet gas may be higher than ~100K if helium thermal "blanketing" effect factored in.

f. H2 recirculation system may be required for propellant supply lines in order to avoid fluid "geysering", unless adequate insulation is provided. Initial analysis suggests that approximately 1" MLI is adequate.

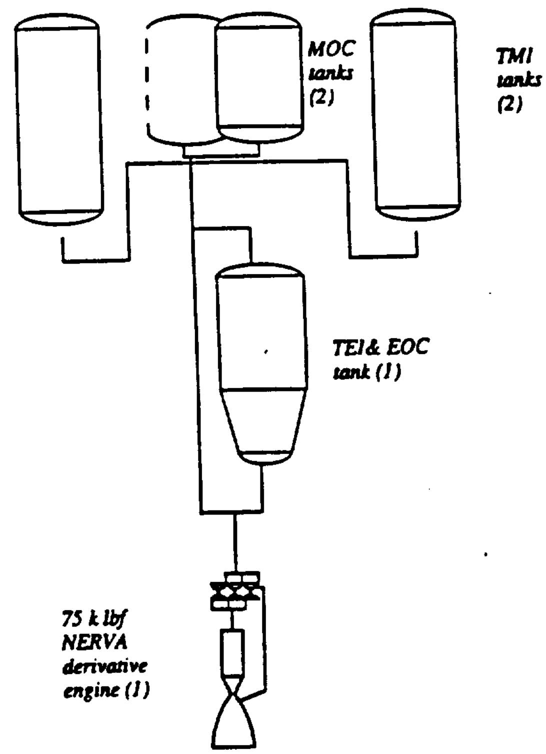

FIGURE 2-1 NTR H_2 PROPELLANT FLOW SCHEMATIC

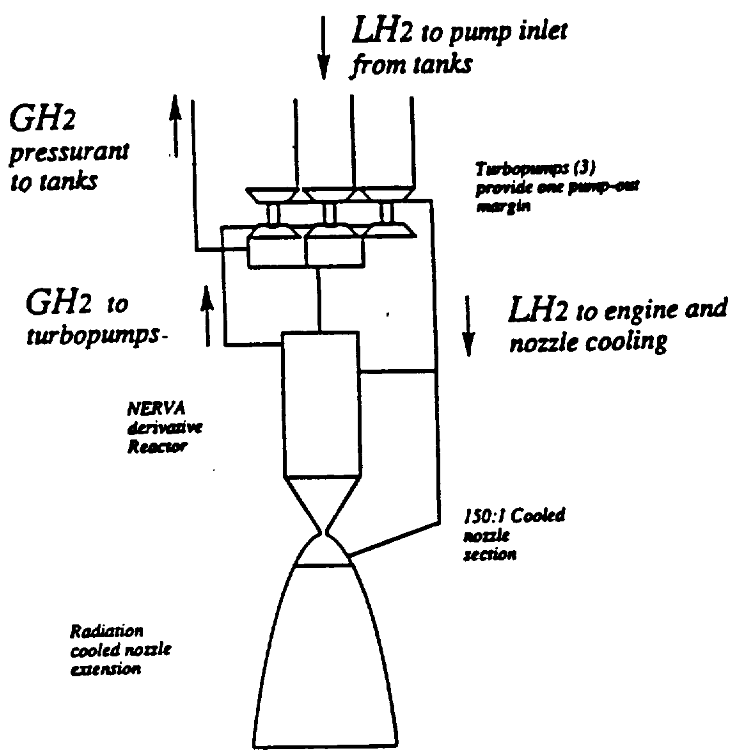

FIGURE 2-2 NTR THREE TURBOPUMP ENGINE SCHEMATIC

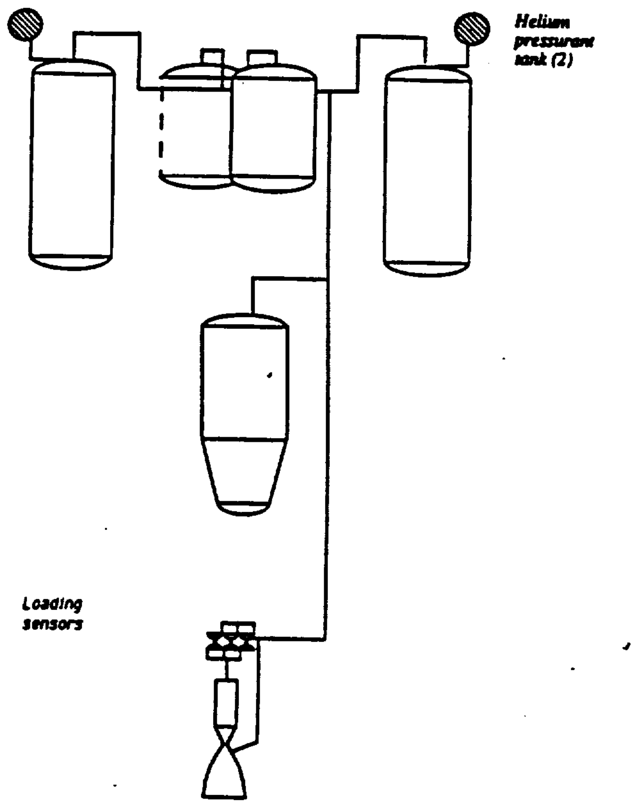

FIGURE 2-3 NTR H_2 AND He GAS TANK PRESSURANT FLOW SCHEMATIC

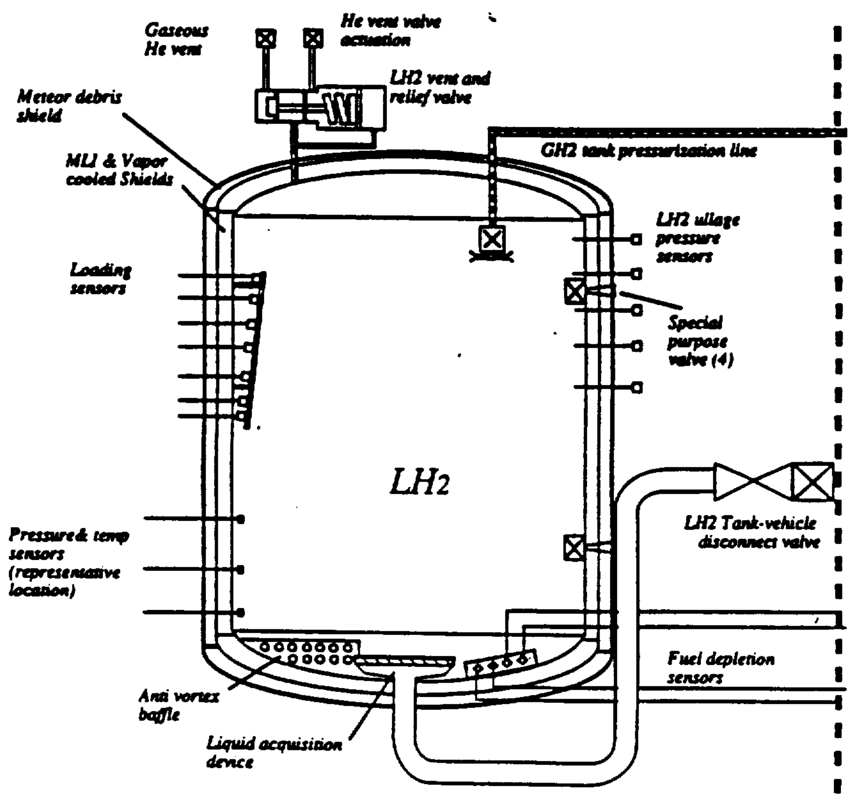

FIGURE 2-4 H_2 TANK SCHEMATIC

Feature	*Primary* Piping	*Secondary* Piping
Purpose	Propulsive thrust	tank pressurant, engine cooling
H2 phases	Liquid and gaseous	gaseous only
Size range	6 to 12 inch	0.5 to 2 inch
Temp range	20 to 180 K	100 to 1200 K
Pressure range	0 to 22 psi	0 to 1000 psi
Flow rate range	0 to 37 kg/sec	0 to 1 kg/sec
General Functions	Prethrust conditioning Propulsive thrust H2 flow Cooldown H2 flow Regenerative cooling H2 fluid transfer	tank pressurant nozzle film cooling RCS thrusting

FIGURE 2-5 FLUID LINE CHARACTERISTICS

Mass flow rate of LH2 = 217.8 kg/sec. Length of LH2 line ~ 100' (30.5 m).

Volume flow rate = 3.085 m^3/sec.

Additional line losses: 4 - 90° bends, 2 - 45° bends, 2 valves, 3 line branches.

Line Dia (cm)	Vel (m/sec)	Re_d	f	$k_{fittings}$	k_{line}	Pdrop (kPa)
30.5 (12")	42.3	17166	.0270	2.36	2.702	319.42
35.6 (14")	31.1	14714	.0277	2.36	2.376	161.31
38.1 (15")	27.1	13734	.028	2.36	2.242	118.94
40.6 (16")	23.8	12875	.0286	2.36	2.146	89.97
43.2 (17")	21.1	12119	.0297	2.36	2.1	69.89
45.7 (18")	18.8	11444	.03	2.36	2.001	54.36
50.8 (20")	15.2	10300	.0305	2.36	1.831	34.27
55.9 (22")	12.6	9363	.0308	2.36	1.68	22.58
61 (24")	10.6	8583	.032	2.36	1.58	15.62
66 (26")	9.01	7923	.0323	2.36	1.492	11.04

FIGURE 2-6 STS PROPELLANT LINE SIZING EXAMPLE

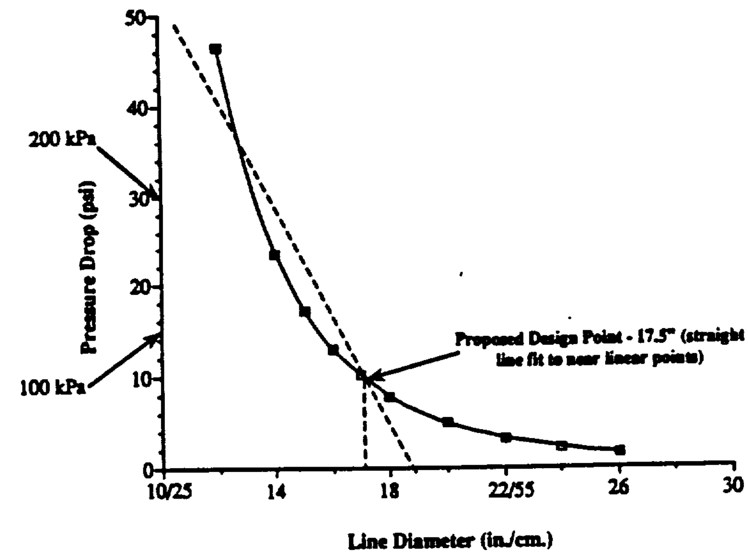

- **Results relatively close to STS actual line diameter (17").**
- **Actual STS line sizing procedure more complicated; Includes iterations due to available fluid acceleration head, turbopump design limitations, standard line sizes, etc.**

NTR Task/jrm/27Feb91

FIGURE 2-7 STS LINE SIZE DETERMINATION EXAMPLE

Mass flow rate of LH2 = 36.8, 73.6, 110.4 kg/sec. Length of LH2 line ~ 40 m.

Volume flow rate = .5213, 1.043, 1.564 m^3/sec.

Additional line losses: 2 - 45° bends, 3 valves, 2 line branches, 1 sharp exit (to aft tank).

Line Dia (cm)	Vel (m/sec)	Re_d	f	$k_{fittings}$	k_{line}	Pdrop (kPa)
2.54 (1")	1029	34805	.023	3.14	36.3	1.05×10^7
5.08 (2")	257.2	17405	,0272	3.14	21.5	5.745×10^4
7.6 (3")	114.3	11602	.03	3.14	15.8	8712.6
10.2 (4")	64.3	8702	.031	3.14	12.2	2238.1
12.7 (5")	41.2	6962	.034	3.14	10.7	827.1
15.2 (6")	28.6	5806	.035	3.14	9.2	355.9
20.3 (8")	16.1	4358	.039	3.14	7.7	99.0
25.4 (10")	10.3	3485 *	.0425	3.14	6.7	36.7
30.5 (12")	7.14	2901*	.044	3.14	5.8	16.1

8", 11", and 13" line sizes selected for 1, 2, and 3 engine cases, respectively.

*** Flow in critical region.**

NTR Task/jrm/27Feb91

FIGURE 2-8 NTR MAIN PROPELLANT LINE DETERMINATION

- 75 klb Thrust Engines -

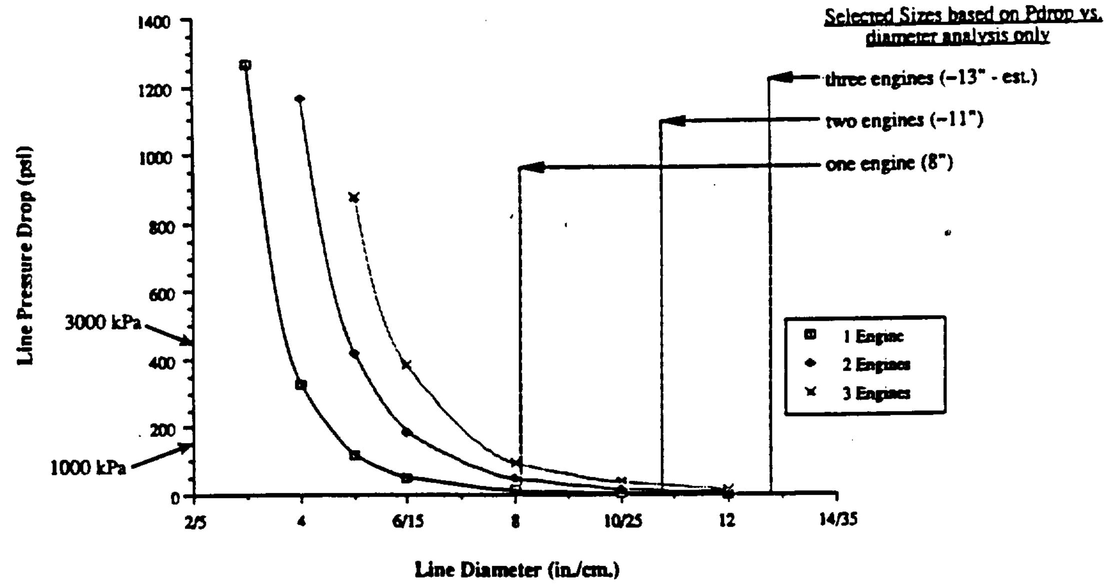

FIGURE 2-9 HYDROGEN LINE SIZING ANALYGIS RESULTS FOR 1, 2, AND 3 ENGINE NTR

Mass flow rate of LH2 = 36.8, 73.6, 110.4 kg/sec. Length of LH2 line ~ 40 m.

Volume flow rate = .5213, 1.043, 1.564 m$_3$/sec.

Additional line losses: 2 - 45° bends, 3 valves, 2 line branches, 1 sharp exit (to aft tank).

Line Dia (cm)	Vel (m/sec)	Red	f	kfittings	kline	Pdrop (kPa)
2.54 (1")	514.3	17401	.027	1.28	21.3	2.104×10^5
5.08 (2")	128.6	8702	.0315	1.28	12.4	8.0×10^3
7.6 (3")	57.2	5801	.036	1.28	9.45	1236.6
10.2 (4")	32.2	4351	.039	1.28	9.0	328.3
12.7 (5")	20.6	3485*	.042	1.28	6.62	118.6
15.2 (6")	14.3	2903*	.044	1.28	5.8	51.0
20.3 (8")	8.04	2176**	.0305	1.28	3.0	9.79
25.4 (10")	5.14	1739 **	.037	1.28	2.91	3.908
30.5 (12")	3.57	1450**	.044	1.28	2.90	1.879

6", 7.5", and 9" line sizes selected for 1, 2, and 3 engine cases, respectively.

* Flow in critical region.
** Flow in laminar region.

NTR Tank/jrm/27Feb91

FIGURE 2-10 NTR TANK PROPELLANT SUPPLY LINE DETERMINATION

- 75 klb Thrust Engines -

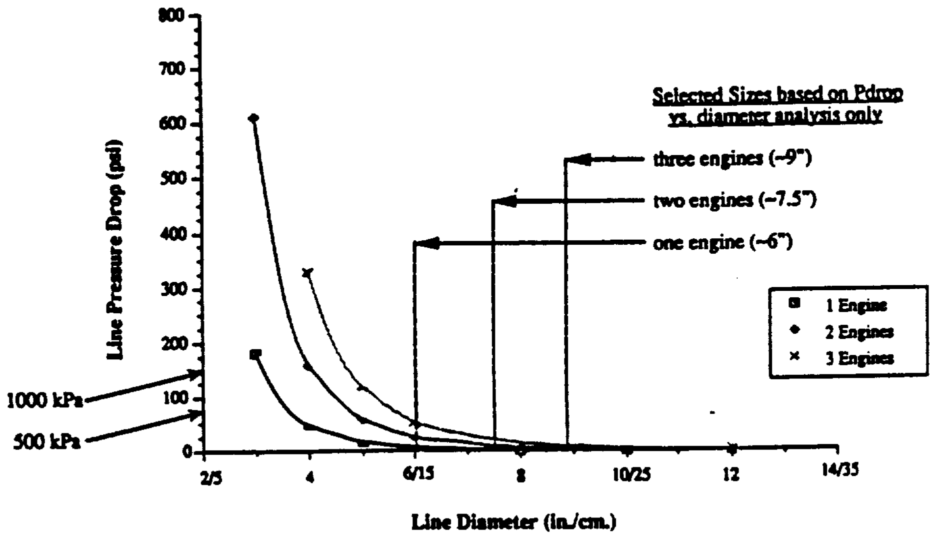

FIGURE 2-11 TMI/MOC TANK LINE SIZING ANALYSIS RESULTS FOR 1, 2, AND 3 ENGINE NTR

Selected Pl = 22 psia. (151.6 kPa.)

Tank Line Dia. (in./cm.)	Delivery Line Dia. (in./cm.)	Pl (psia./kPa.)
4 / 10	8 / 20	74.3 / 512.1
6 / 15	8 / 20	37.9 / 261.2
6 / 15	10 / 25	29.6 / 203.8
6 / 15	12 / 30	26.8 / 184.9*
8 / 20	8 / 20	32.5 / 224.4
8 / 20	10 / 25	24.2 / 167.0*
8 / 20	12 / 30	21.5 / 148.1*
10 / 25	10 / 25	23.5 / 162.3*
10 / 25	12 / 30	20.8 / 143.5*

* Denotes acceptable candidate line size combination.

FIGURE 2-12 FINAL LINE SIZING ANALYSIS BASED ON ALLOWABLE PRESSURE DROP

3. AEROBRAKE INTEGRATION

During the current technical directive, the study addressed materials and structural concepts for the aerobrake. The initial work is being performed for the L/D=0.5 aerobrake configuration which was developed in the Phase I work.

3.1 Properties and Processing of Intermetallic Titanium Aluminides

3.1.1 Abstract

Although full maturity of the technology is at least ten years in the future, intermetallic titanium aluminide-based alloys are expected to compare favorably against superalloys in weight critical aerospace structures where high temperature strength, high elastic modulus, and resistance to oxidation is required. Titanium aluminides have been suggested for a reusable Mars excursion vehicle (MEV) for precisely these reasons (Reference 3-1). Successful use of titanium aluminides in such applications requires a detailed understanding of material properties and limitations. The focus of this study has been to examine the properties and processing characteristics of these materials with a goal of identifying specific technology development needs.

3.1.2 Introduction

Intermetallic phases within the titanium-aluminum system have been known to exist for over 30 years (Reference 3-2). In many applications, these hard, brittle compounds were considered undesirable because they tend to form at grain boundaries causing a reduction in toughness and ductility. Similarly, titanium alloys reinforced with alumina ceramic fibers resulted in brittle failure of titanium aluminide intermetallic compounds at the fiber/matrix interface. Since about 1973, however, titanium aluminides have been under investigation for their potential use in lieu of nickel-based superalloys in aircraft turbine engines and hypersonic vehicle structures. Work has focused both on dispersion strengthening of titanium matrices by precipitation of intermetallic phases and upon creation of new structural alloys based on titanium aluminide intermetallic compounds.

Atomic bonding in titanium aluminide intermetallics is not entirely metallic in nature; there is a degree of covalent character such that the valency electrons are not entirely mobile within the material. The electrons may be considered to be constrained within a specific lattice by hybridization of titanium's 3p and 4s orbitals. This hybridization of bonds is believed to contribute to lattice ordering which is a major factor explaining the high temperature strength and stiffness of titanium aluminide compounds.

3.1.3 Alloying Elements and Their Effects

Commercially pure titanium is an allotropic material, existing in the HCP lattice structure (alpha phase) below 882°C and BCC lattice structure (beta phase) above 882°C. Alloying elements are added to titanium primarily for three reasons: 1) to change the phase transformation temperature and thereby stabilize or adjust the relative amount of each phase present: 2) to cause solution strengthening or improve the martensitic hardenability of the resulting alloy; and 3) to improve some specific property such as oxidation or corrosion resistance. Aluminum has long been an important alloying element in commercial titanium alloys. Addition of aluminum in the range of 20-50 atomic percent aluminum (10-35 weight per cent aluminum) provides solution strengthening and significantly increases the transformation temperature (beta transus). The titanium-aluminum equilibrium phase diagram, as it is currently understood, is shown in Figure 3.1 (Reference 3-3).

Substitutional alloying elements perform essentially the same function in titanium aluminides as in conventional (disordered) titanium alloys, such as Ti-6Al-4V, if they do not enter into the ordering reaction to a significant degree. Tantalum, vanadium, and niobium are the preferred substitutional beta stabilizers because they are isomorphous the beta phase titanium. The addition of vanadium makes complete beta-to-alpha transformation upon cooling impossible and therefore can be used to control the portion of beta phase which is stable at room temperature. Zirconium is unique in that it is isomorphous with both the alpha and beta phases of titanium and may be used to solution strengthen titanium alloys without affecting the transformation temperature. Niobium, vanadium, and molybdenum are often used to improve both strength and oxidation resistance of titanium alloys (Reference 3-4).

3.1.4 Properties of Titanium Aluminide Intermetallics

Of the four intermetallic phases depicted on the titanium-aluminum equilibrium phase diagram (Ti_3Al, TiAl, $TiAl_2$, and $TiAl_3$), only alpha-2 (Ti_3Al) and gamma (TiAl) based alloys are presently considered to have commercial significance. The others have not proven feasible to produce using current processing practices due to the narrow composition ranges over which they exist and their high rate of strain hardening. Since alpha-2 and gamma based alloys are the focus of the majority of titanium aluminide research, the majority of this study is directed toward the characteristics of these compounds. Some of the relevant properties of alpha-2 and gamma titanium aluminides in comparison with a conventional Ti-6Al-4V alloy are summarized in Figure 3-2 (References 3-4, 5, 6, 12 & 13).

a. Yield Strength and Elastic Modulus - The high yield strength and elastic modulus which is characteristic of titanium aluminide compounds at temperatures approaching approximately one-half their melting point (Tm) is believed to depend upon the degree of long range ordering. Ordering leads to somewhat stronger atomic bonding; the strength of these bonds being proportional to elastic modulus. But perhaps a more significant factor affecting mechanical properties is the behavior of crystalline defects known as anti-phase domains. In both alpha-2 and gamma titanium aluminides, anti-phase domains may consist of stacking faults as well as unfavorable atomic interactions between "nearest neighbor" or "next nearest neighbor" atoms. Compared to randomly dispersed solid solutions of similar composition, ordered intermetallic compounds exhibit a high degree of resistance to slip. Anti-phase domains play an important role in this behavior. However, mechanisms by which this occurs are not fully understood (References 3-7 and 3-8).

b. Ductility and Fracture Behavior - Titanium aluminides are notoriously brittle at ambient to moderate operating temperatures. The elongation of alpha-2 compounds is only about 2% at temperatures below approximately 0.5Tm. Thus far, a maximum of about 5% elongation in this temperature range has been achieved by modifying the compound. The brittleness of ordered alloys is attributed to a lack of sufficient slip systems to permit deformation at the grain boundaries. Studies of other aluminide compounds indicate that ductility is strongly dependent upon the superlattice structure and mildly dependent upon the degree of long range ordering. Fracture of intermetallic compounds most frequently results from intergranular clevage arising from a build up of dislocation strain energy.

Above approximately 0.5Tm, increased cross slip, dislocation climb, and other thermally activated dislocation activity results in higher ductility. Consequently, a brittle-to-ductile transition is observed. Methods of improving the low temperature ductility of ordered materials include the selective use of alloying elements, control of grain size, and thermo-mechnical processing techniques. The addition of small quantities of niobium, for example, is found to reduce the brittle-to-ductile transition temperature of Ti_3Al to about

600°C by the formation of Nb_2Al. The success of alloying elements in improving low temperature ductility is believed to lie in the ability of favorable constituents to segregate to grain boundaries and relieve localized strain. Dispersions of niobium aluminides are thought to enhance titanium aluminides by this mechanism (Reference 3-9). Improving the ductility of intermetallic materials at low to moderate operating temperatures continues to be the subject of intensive research.

c. Oxidation Resistance - The oxidation resistance of aluminide compounds is high because all of these compounds contain a large atomic fraction of aluminum. The higher the aluminum content, the higher the oxidation resistance. For this reason, the $TiAl_3$ compound has been suggested for use as an oxidation resistant coating material for other titanium aluminide compounds. Aluminizing of titanium aluminides might be accomplished by thermal spraying, molter metal dipping, or pack cementation. Upon exposure to high temperature oxidizing environment, titanium aluminides readily form an adherent titania (TiO_2) and/or alumina (Al_2O_3) scale which protects the substrate alloy from further oxidation, see Figure 3-3 (Reference 3-10). Certain alloying agents such as niobium, when added in sufficient quantity have been shown to improve oxidation resistance up to 850°C by entering into ternary reactions which promote the formation of titania and alumina products.

d. Strain Hardening - Long range ordered alloys usually exhibit high strain hardening rates compared to their disordered counterparts, making them extremely difficult to process. However, in the Ti_3Al lattice, the strain hardening rate is substantially unaffected by temperature up to about 700°C. Studies show that the strain hardenability of gamma Ti_3Al + Mo alloys increases proportionally with stress amplitude below 700°C by a build up of planar bands of basal dislocations (Reference 3-11). The role of superlattice dislocations in strain hardening is the subject of ongoing investigations, but the strain hardening phenomena of Ti_3Al enables the alloy to be strengthened by thermo-mechanical processing techniques which are similar to conventional methods. Strain hardening is also expected to improve erosion resistance of intermetallic alloys, in some cases abrigating the need for protective surface coatings.

3.1.5 Fabrication and Processing Techniques

Alloys based on alpha-2 titanium aluminides are now being demonstrated in a wide variety of parts utilizing both conventional and innovative new manufacturing technologies.

Research and development for specific applications is continuing at the Air Force Wright Aeronautical laboratory and at numerous aerospace companies. Some of the applications which have been demonstrated are listed in Figure 3-4 (References 3-3, 3-5 & 3-14). The basic difficulty being experienced in development are problems of reproducibility and homogeneity. Titanium aluminides are more sensitive to property variations as a result of small changes in composition or processing conditions than conventional alloys, and are therefore more difficult and more expensive to process.

Bulk form titanium aluminides are normally obtained by powder metal processing (e.g. hot isostatic pressing), or by vacuum arc melting and casting. Forming may be accomplished by high temperature extrusion or a procedure of repeated cold rolling and recrystallization to sequentially reduce gauge thickness. Rapid solidification techniques, such as drop casting and melt spinning, have been successfully used to refine grain size and limit segregation during solidification. As might be expected, intermetallic alloys are difficult to forge. Additions of reactive alloying elements are being investigated to improve hot formability and reduce sensitivity to metallurgical impurities and contamination.

3.1.6 Summary and Conclusions

In summary, intermetallic phases of titanium aluminide which have been known to exist since the early days of titanium metallurgy are now being developed for applications in high temperature aircraft turbine engine and hypersonic vehicle structures. Very low ductility at ambient to moderate operating temperatures continues to be the major obstacle to their widespread use. Metallurgical engineers are actively pursuing research related to deformation behavior, with a goal of designing new alloys which overcome the inherent limitations of this class of materials. Selective use of alloying elements, grain size control, and thermo-mechanical processing techniques are the primary means of modifying material behavior. However, most properties and characteristics are directly attributed to the basic lattice composition and structure.

Fabrication technologies using alloys based on alpha-2 titanium aluminides are currently being demonstrated in prototype hardware. Many of the conventional processing methodologies may be adapted to these ordered compounds, but careful attention must be paid to process control in order to minimize variability of physical properties in the finished product. Difficulties in fabrication make titanium aluminide parts very expensive to produce. Nevertheless, the trend towards higher performance in weight critical aerospace applications makes continued development imperative.

3.2 Aerobrake Structural Integration

A total of nine tasks are planned for developing and trading aerobrake structural configurations. Three of the tasks, literature survey, preliminary sizing, and analysis tool reviews were completed for one configuration of the aerobrake. The fourth task, which included constructing a preliminary finite element model, was initiated. The remaining tasks relate to the analysis, optimization and structural design for the configuration.

Groundrules and assumptions which were established prior to task commencement are as follows:

a. The baseline aerobrake geometry is the current Boeing L/D 0.5 aerobrake concept.

b. Payload (MEV) mass is 83 metric tonnes.

c. Maximum deceleration (during aerocapture maneuver) is 6g at a relative wind angle, RWA = 20 degrees.

d. 6g aerocapture is worst case.

e. Three to five structural concepts will be analyzed and developed for minimum mass.

f. Material selections will be based on concurrent, independent trades and technology projections which are optimized for each structural concept being considered.

The specific task results are discussed below.

a. Task 1, Literature Review - Aerobrake structural work performed by North Carolina State University and NASA Langley Research Center was reviewed to ensure that there would be no unnecessary duplication of effort. It was determined that, due to differences in assumptions and aerobrake geometry and structural concepts, the previous work was incomplete and did not provide enough evidence for trading all current concepts.

b. Task 2, Design Configuration - The first concept chosen for analysis consists of a semi-monocoque shell of sandwich construction with advanced composite / laminate materials. For purposes of preliminary sizing for inclusion in the initial finite element model, the shell was assumed to be a monolithic shell of spherical section. The material was assumed to be titanium. A uniform sandwich configuration was then developed which provides stiffness equivalent to the monolithic shell at a reduced weight.

c. Task 3, Design Simulations - The capabilities and limitations of ANSYS and NASTRAN finite element programs were reviewed to evaluate their suitability for performing stress analysis of aerobrake structures. Specifically, the available finite elements and program features will be considered in selecting an appropriate program for mathematical simulation and analysis of the aerobrake structures.

The ANSYS program has beam, shell, solid, and composite elements to simulate different design configurations. It also has compatible thermal elements to perform coupled thermal/stress analyses. The following are applicable elements for aerobrake application.

(1) 3-D spar, STIF8
(2) 3-D beam, STIF4
(3) 3-D plastic shell, STIF43
(4) 3-D quadrilateral shell, STIF63
(5) Isoparametric shell, STIF93
(6) Isoparametric solid, STIF45
(7) Anisotropic solid, STIF64
(8) Layered composite shell, STIF91 and STIF99
(9) Layered composite solid, STIF46
(10) Reinforced composite solid, STIF65

Combinations of the above elements will be used to simulate different design configurations such as monocoque shell, space frame, stiffened semi-monocoque shell, etc. The layered elements will be used for composite material applications. The capabilities and features of each element are summarized in Figure 3-5.

Nastran has the following elements for modeling aerobrake structures:

a. CBEAM
b. Triangular shell, CTRIA3 and CTRIA6
c. Quadrilateral shell, CQUAD4 and CQUAD8
d. Solids, CHEX20

The Nastran elements are similar to ANSYS elements except that they do not support orthotropic materials. These elements lack other options also, including large deflection, stress stiffening, and variable element thicknesses but are still sufficient for simulating the expected aerobrake structural elements. The Nastran program does not provide a wide choice of elements for modeling composite materials as ANSYS does. A summary of Nastran element features is given in Figure 3-6.

In summary, both ANSYS and Nastran elements can adequately be used in developing finite element models of the aerobrake structures. ANSYS, however, has elements more suitable for modeling composite materials. It also has extensive pre/post-processing capabilities which Nastran lacks. Other useful features of ANSYS include design optimization and a larger element library compred to Nastran and may therefore be a better choice to model and analyze aerobrake structures.

d. Task 4, Preliminary Finite Element Model - Due to its immediate availability, IDEAS Supertab was used for pre-processing and preparation of the initial aerobrake model. This model will be converted to ANSYS for analysis and subsequent iterations and/or modifications.

The preliminary model consists of thin shell elements which define the aerobrake geometry. These elements are loaded by element face pressures as calculated in an separate aerodynamics analysis. The pressure loading is variable and ranges from 0 at the aft lip section to 13,675 Pascals at the stagnation point. The loaded model is shown in Figure 3-7. Note that the pressure vectors do not represent magnitudes and are not scaled. A scaled left-side and front views of the pressure distributions are shown in Figure 3-8.

Physical and material properties are being finalized for inclusion in the model.

REFERENCES

3.1 Boeing Aerospace and Electronics, NASA Contract NAS8-37857, Space Transfer Concepts and Analysis for Exploration Missions, 4th Quarterly Review, Oct. 17, 1990, pp. 4-32 - 4-35.

3.2 The use of the term "intermetallic" is the subject of some controversy. For purposes of this text, all intermediate phases which exhibit a intermediate to long range ordering and a degree of covalent bonding behavior shall be regarded as "intermetallic".

3.3 R. N. Boggs, ed., "Titanium Aluminide: True Space-Age Material," Design News, Cahners Publishing Co., June 19, 1989, reprint edition.

3.4 H. E. Boyer and T. L. Gall, eds., Metals Handbook, Desk Edition, (Metals Park, Ohio: American Society for Metals, 1985), p. 9-2.

3.5 H. A. Lipsitt, "Titanium Aluminides - An Overview" High Temperature Ordered Intermetallic Alloys, Materials Research Society symposia proceedings, Vol. 39, (Pittsburgh, PA: Materials Research Society, 1985), pp.351-364.

3.6 Texas Instruments, "Ti Aluminide Data Sheet," Rev. 3, March 28, 1990.

3.7 D. Shechtman, M. J. Blackburn, and H. A. Lipsitt, "The Plastic Deformation of TiAl," Met. Trans., Vol. 5, 1973, P. 1373.

3.8 S. M. L. Sastry and H. A. Lipsitt, "Plastic Deformation of TiAl and Ti_3Al," Proceedings of the 4th International Conference on Titanium, Japan, Nov. 1980, P. 1231.

3.9 N. S. Stoloff, "Ordered Alloys for High Temperature Applications," High Temperature ordered Intermetallic Alloys, Materials Research Society symposia proceedings, Vol. 39, (Pittsburgh, PA: Materials Research Society, 1985), PP. 3-27.

3.10 M. Yamaguchi, U. Umakoshi, and T. Yamane, "Deformation of the Intermetallic Compound Al3Ti and Some Alloys with An Al^3Ti Base," High Temperature Ordered Intermetallic Alloys II, Materials Research Society symposia proceedings, Vol. 81, (Pittsburgh, PA: Materials Research Society, 1987), pp. 275-286.

3.11 N. S. Stoloff, et al., "Fatigue of Intermetallic Compounds," High Temperature Ordered Intermetallic Alloys II, Materials Research Society symposia proceedings, Vol. 81, (Pittsburgh, PA: Materials Research Society, 1987), pp. 247-261.

3.12 J. Rosler, et. al., "The High Temperature Behavior of TiAl Containing Carbide Reinforcements," Intermetallic Matrix Composites, Materials Research Society symposia proceedings, Vol. 194, (Pittsburgh, PA: Materials Research Society, 1990), pp. 241-248.

3.13 MIL-HDBK-5E, Metallic Materials and Elements for Aerospace Vehicle Structures, Vol. 2, (Washington, D.C.: USAF, 1987, p. 5-55.

3.14 L. Kempfer, ed., "Materials Take a Hypersonic Leap Into Space," Materials Engineering, Penton Publishing, Cleveland, OH, August 1990, pp. 19-22.

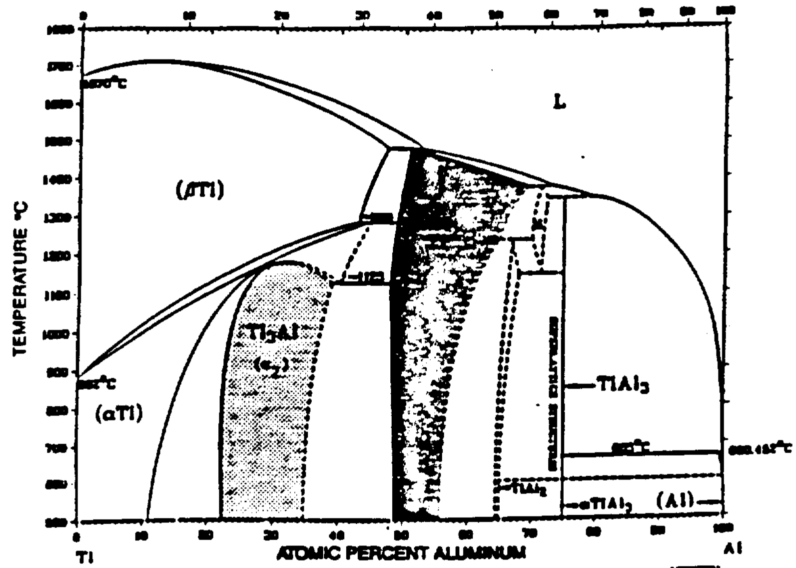

FIGURE 3-1 TITANIUM-ALUMINUM EQUILIBRIUM DIAGRAM SHOWING THE TWO MOST IMPORTANT ALUMINIDES: ALPHA-2 AND GAMMA 3

Property	Ti-6Al-4V (alpha+beta)	Ti3Al +Nb(alpha-2) (alpha-2+beta)	TiAl+C(gamma) (gamma+Ti AlC)
Density (g/cc)	4.5	4.2 - 4.7	3.7 - 3.9
Melting Temp. (°C) (pure compound)	1700	1600	1460
Max. Temp for Creep (°C)	538	815	1038
Max. Temp for Oxidation (°C)	593	649	1038
Ductile-to-Brittle Transition (°C)	n/a	600 - 760	600 - 700
UTS (25°C)	1100	940	**
(MPa) (700°C)	n/a	750	**
0.2% Offset (25°C)	980	830	640
YS (MPa) (700°C)	n/a	810	640
Elast. Mod. (GPa)	96 - 100	110 - 145	176
Elongation (%)			
(circa 25°C)	20+%	2 - 5%	1 - 2%
(circa 0.5Tm)	high	5 - 8%	7 - 12%

Note: Properties reflect information available on optimized alloys and processing methods.
n/a = not applicable; ** = data unavailable
Sources: [4,5,6,12,13]

FIGURE 3-2 TYPICAL PROPERTIES OF TITANIUM ALUMINIDE ALLOYS VS. CONVENTIONAL TITANIUM Ti-6Al-4V ALLOY

FIGURE 3-3 SCANNING ELECTRON MICROGRAPH SHOWING A CROSS SECTION OF THE OXIDE SCALE ON TiAl AFTER EXPOSURE TO AIR AT 900°C FOR 200 HOURS

Investigating Company/Agency	Fabrication Methods(s)	Structure/ Component(s)
AFWAL	Forging Billet Sheet Rolling Casting, Machining	Tech. Demonstration
AFWAL	Rolled Ring Forging	Turbine Stator Support Rings (45 cm dia.)
AFWAL	Rolled Ring Forging	Compressor Section Casing (50 cm dia.)
AFWAL	Precision Casting	Turbine Blades
AFWAL, Boeing	Superplastic Forming/ Diffusion Bonding	Afterburner Divergent Nozzle Seal, Aircraft Wing Stiffeners
McDonnell-Douglas/ Textron	Diffusion Bonding/ Composite Structure	NASP Structural Skin
Texas Instruments/Rohr	Cold Rolling (foil)	Honeycomb Core

Sources: [3,5,14]

FIGURE 3-4 TITANIUM-ALUMINIDE TECHNOLOGY DEMONSTRATIONS

Element	No. of Nodes	Degrees of Freedom	Material	Element Loading	Thermal Element	Special Features	Application
STIF4, 3-D Beam	2	UX, UY, UZ RX, RY, RZ	Is	Pressure or linear temp. gradients	-	Tapered cross sec., nodal offsets, shear deflection, initial strain, S, R	3D truss, frame or stiffener with tension, compr., & bending
STIF8, 3-D Spar	2	UX, UY, UZ	Is	Nodal temp & force	-	Uniaxial tension-compr, P, R, S	Truss, spring
STIF43, Plastic Quadrilateral Shell	4	UX, UY, UZ RX, RY, RZ	Is, Or	T, P	STIF57	Variable thickness membrane & bending stiffness, P, R, S, plasticity can be turned off.	Nonlinear, flat or warped thin to moderately thick shell.
STIF63, Elastic Quadrilateral Shell	4	UX, UY, UZ RX, RY, RZ	Is, Or	T, P	STIF57	Variable thickness, membrane and/or bending stiffness, reduced mass matrix option, extra displacement shape suppression option, R, S	Thin to moderately thick elastic shell
STIF93, Isoparametric Shell	8	UX, UY, UZ RX, RY, RZ	Is, Or	T, PR	STIF57	Variable thickness, P, R, S	Curved shell

Element	No. of Nodes	Degrees of Freedom	Material	Element Loading	Thermal Element	Special Features	Application
STIF45, Isoparametric Shell	8	UX, UY, UZ RX, RY, RZ	Is, Or	NT, PR	STIF70	P, R, S	3D solid modeling
STIF64, Anisotropic Solid	8	UX, UY, UZ RX, RY, RZ	AN	NT, PR	STIF70	Anisotropic or crystalline materials	Solid modeling of anisotropic material
STIF91, or STIF99 Layered Shell	8	UX, UY, UZ	Is, Or	T, PR NT	-	Up to 16 layers & material properties in STIF91 & up to 100 layers in STIF99, no slippage between layers variable layer thickness	Layered composite shell
STIF46, Layered Solid	8	UX, UY, UZ	Is, Or	T, PR NT	-	up to 100 layers, material layer proper by orientation option, no slippage between layers	Thick layered composite shell or solid
STIF65, Reinforced Solid	8	UX, UY, UZ	Is	NT, PR	-	One solid and up to 3 rebars,capable of cracking in tension and crushing in compression, nonlinear material proper by specification, plasticity	Modeling of reinforced composite thick shells or solids

FIGURE 3-5 FEATURES AND CAPABILITIES OF SELECTED ANAYS ELEMENTS

Element	No. of Nodes	Degrees of Freedom	Material	Element Loading	Thermal Element	Special Features	Application
CBEAM	2	UX, UY, UZ RX, RY, RZ	Is	Pressure or thermal gradient	-	Tapered cross section, nodal offsets	3D truss frame or stiffener
CTRIA3/ CTRIA6 Shell	3	UX, UY, UZ RX, RY, RZ	IS, AN	T, PR	Y	P, CTRIA has optional mid side node, optional coupling of bending and membrane stiffness	Thin to moderately thick shell
CQUAD4/ CQUAD8 Shell	4/8	UX, UY, UZ RX, RY, RZ	IS, AN	T, PR	Y	P, CQUAD8 has optional mid side node, optional bending and membrane stiffness coupling	Thin to moderately thick shell
CHEX20 Solid	8 or 20	UX, UY, UZ RX, RY, RZ	IS, AN	T, PR	Y	P	Solid modeling, thick shell

IS = Isotropic
OR = Orthotropic
AN = Anisotropic

T = Surface tempreture
PR = Surface pressure
NT = Nodal tempreture

P = Plasticity
R = Large Deflection
S = Stress stiffening

FIGURE 3-6 FEATURES AND CAPABILITIES OF SELECTED NASTRAN ELEMENTS

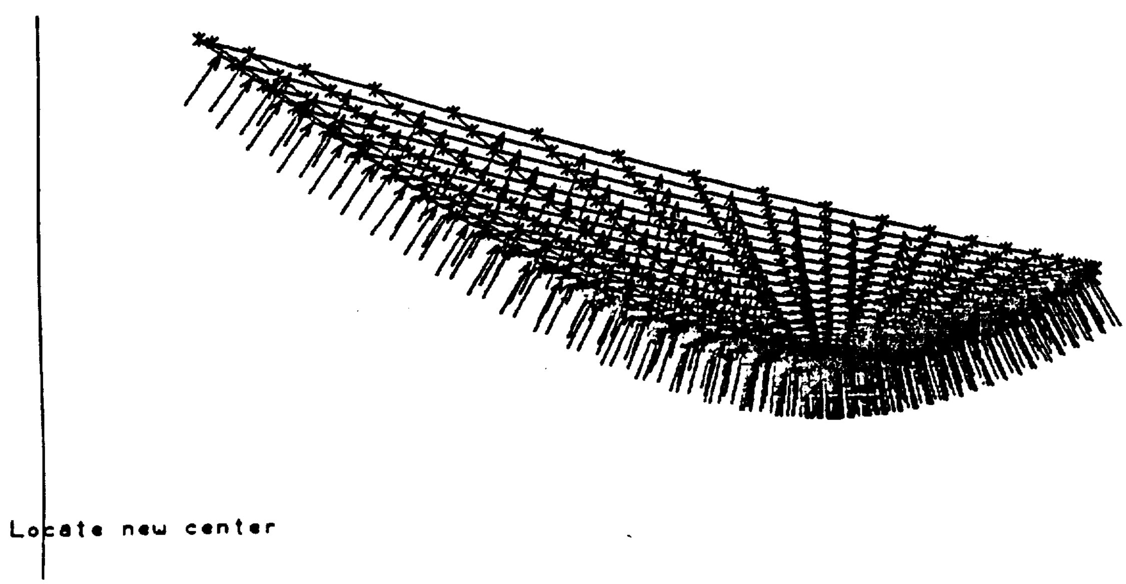

FIGURE 3-7 FINITE ELEMENT MODEL WITH LOADS

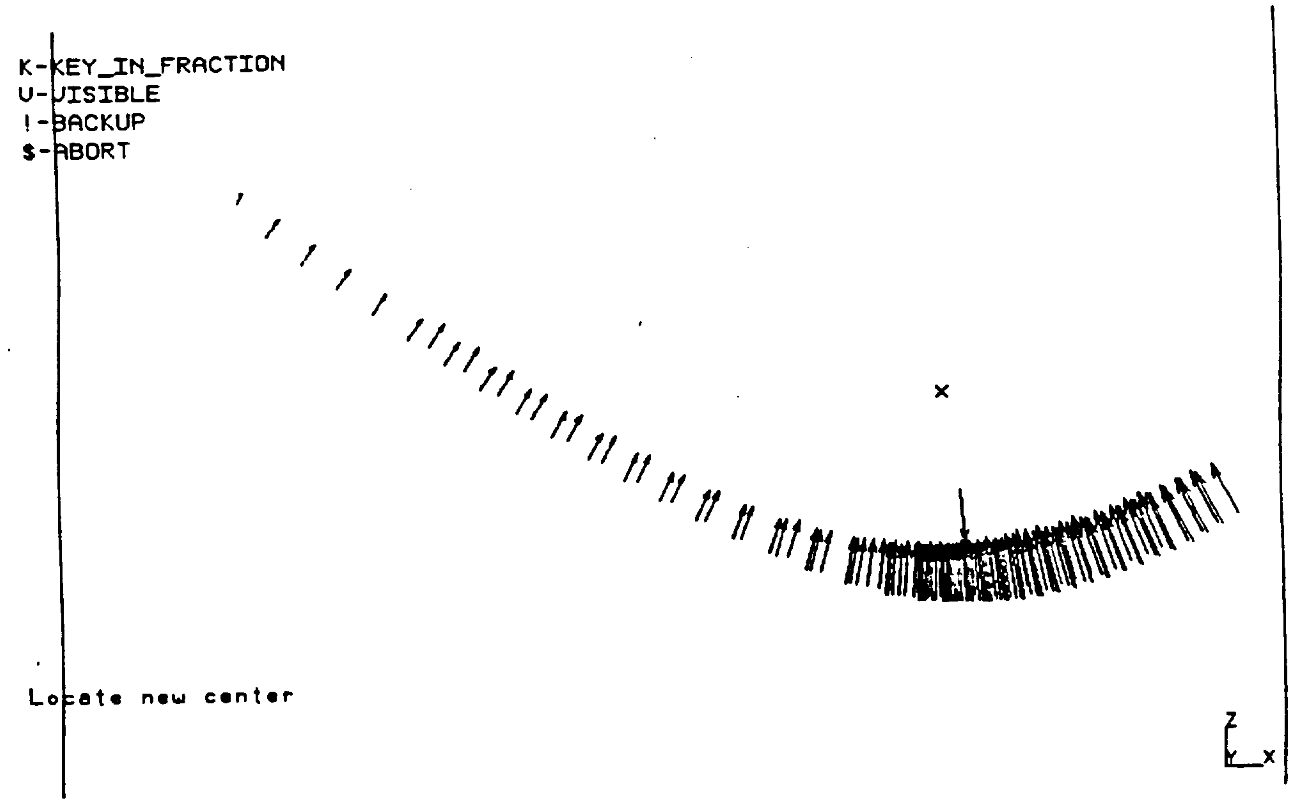

FIGURE 3-8A SCALED LOAD VECTORS, LEFT SIDE VIEW

FIGURE 3-8B SCALED LOAD VECTORS, FRONT VIEW

4. Assembly Operations and ETO Vehicle Size Requirements

Within this Phase II section of the STCAEM study, initial on-orbit assembly systems for the NTR vehicle were evaluated for continued study in the Phase III portion of the contract. To the set of assembly platforms that were generated in the first phase of the contract, (Figures 4.1 - 4.2) several additional concepts were added. A brief discussion of these concepts are provided.

4.1 Gantry-Rail Platform

This configuration allows access to all parts of the vehicle and gantry with storage and support platforms to be attached to the upper surface of the rail away from the vehicle (no interference with the track), Figure 4-3. The vehicle is held by standoffs from the rail which may be easily removed after vehicle departure. The mobile gantry is large enough to clear all parts of the vehicle including the tanks and aerobrake. The rail itself is a reinforced, but still light truss-type structure. The First Element Launch (FEL) will be required to deploy, assemble the system and make it operational.

The concerns are:

(1) The gantry may have to be counter balanced (storage platform may help here).

(2) There may be a vehicle balance problem (again storage platforms may help).

(3) The rail will have to be stiff to keep the gantry centered.

(4) Detachment of the vehicle from the platform will require some delicate maneuver capability on both the vehicle and platforms' parts.

(5) The rail joint-truss release my not be simple.

The advantages are:

(1) It is a relatively simple platform.

(2) It has low mass.

(3) The attachment points are generally simple.

(4) It has full access to the length and circumference of the vehicle.

(5) It can be reused easily or be used for other purposes on orbit.

4.2 Modified I-Beam with Lazy Susan

This is the same configuration described by the Phase I I-Beam arrangement with the addition of the turntable that attaches between the vehicle truss and the platform central beam, Figure 4-4. All the advantages and disadvantages of the I-Beam form are present with the addition of an extended reach advantage at the price of some complication in the "lazy susan" turntable.

4.3 Common Hab and Assembler/Servicer

This configuration involves modifying a pressurized MTV crew habitat with an ACRV and airlock by reinforcing the end domes and attaching robotic arms to them and reinforcing a circumference panel to accept an articulated RMS arm and power/control cable, Figure 4-5. It attaches to the NTR truss by the circumference panel RMS and maneuvers around the vehicle and along the truss. It is crew controled and will run off the vehicle facilities. A FEL will be required to initiate the operations.

The concerns are:

a. It requires a redesign of the NTR MTV habitat.

b. The complexity of the habitat increases greatly.

c. Manipulating the robot arms with limited visibility may be a sensitive operation.

d. It is almost free floating and when maneuvering objects, particularly massive ones, will have to be secured.

e. It has very limited storage.

f. It may increase orbital operations time.

g. It may have limited reuseability.

h. It requires extensive crew involvement in the operations.

i. It may require early launch of auxiliary or disposable systems such as power (arrays).

The advantages are:

a. No unnecessary infrastructure.

b. The assembly crew is present during operations.

c. The Assembly/Servicer may or may not be used as the MTV Transit Hab.

4.4 Tethered Robotic Assembly Platform

This platform consists of a long beam perpendicular to the NTR truss that has a continuous tether system anchored off the ends of the NTR truss, Figure 4-6. At least a pair of, possibly four, mobile RMS robots travel along the tether to pick up parts stored on the beam and assemble the vehicle. These robots can rotate about the tether. The beam is long enough to allow the robots to clear the tanks. The power is supplied to the robots by batteries that are recharged from the platform main power supply. The tether truss is deployable, but an FEL mission is necessary to deploy the vehicle truss with GN&C, communications and reboost RCS, attach the central truss and deploy the solar array, attach the tether system and the MTV habitat module and attach berthing and storage fixtures. Localized debris shielding will be used on the vehicle to protect it. The tether and tether beam can be removed from the vehicle and stored on orbit.

The concerns are:

a. Refurbishment of the vehicle systems prior to departure may be difficult.

b. Vibrations on the tether may interfere with robot movement and operations.

c. Large objects cannot be stored on the tether, and the storage on the beam is limited.

d. CTV and delivery vehicle docking or berthing will be delicate operations.

e. Placement of the solar arrays is still an open question.

f. The EVA requirements are undefined but likely to be large.

g. The mode of on orbit storage is still undefined.

h. The length of the central beam is over 100 meters.

The advantages are:

a. It is a deployable structure.

b. It can be discarded after the vehicle assembly is complete.

c. It could be launched in one flight.

d. It will likely have relatively low cost.

4.5 Assembly Ball Platform Concept

This is an assembly box similar to the gantry in the Gantry -Rail Platform design, except that there is no rail and the gantry is mobile on the NTR truss itself, Figure 4-7. The assembly ball is self contained in power, thermal control, communications and storage. The robotic arms are mobile over the lip of the ball therefore they can work inside or outside the ball. The concerns and advantages are shown in Figure 4-8.

4.6 H-O Assembly Platform Concept

This platform is a large strong truss structure that is a modified Gantry -Rail Platform with a large attached non-mobile truss bay opposite the vehicle assembly area and no mobile gantry, Figure 4-9. The function of the mobile gentry is taken up by the platform robotics for component placement after the component has been assembled in the bay area. The concerns and advantages are shown in Figure 4-10.

4.7 General Requirements

All the assembly platforms will fly in a gravity gradient stabilized mode. These were evaluated against a set of known requirements and common sense criteria. The known requirements must be satisfied either by the platform itself or a combination of the vehicle and platform together. There is the tendency to burden the platform with most of the shared needs in order to prevent degradation of critical Mars vehicle systems. Core requirements that must be satisfied are: the ability of the platform-vehicle to have reboost capability for orbit maintenance, GNC and communications station (EVA and robotic), storage space for equipment not in use and parts, berthing space for a CTV (cargo transport vehicle) and/or the delivery vehicle, sufficient power and power distribution prior to, during and after the vehicle is at the platform, adequate lighting for both robotic operations and EVA including transition in occultation, thermal control for the platform (perhaps temporary for the vehicle) equipment, accessibility both by EVA and robotic arms to all portions of the vehicle, robotic arms for assembly operations, position reference sensors for platform/ robot/ vehicle relative positioning, vehicle and equipment tie-downs to the platform, EVA tie-downs, local or global debris shielding, EVA housing for astronauts working around the vehicle-platform (may be provided by the CTV) and safety /escape provisions for these astronauts. These requirements had to be judged in the light of reasonable expectations of program and vehicle demands. That is, we could not expect to have the platform and its construction put a demand on the development costs, launch schedule and complexity or the on-orbit operations equal in magnitude to the construction of the Space Station, neither could a platform system be inflexible to the point of excluding the known NTR vehicle design set nor create a major impact to the top-level NTR configurations. These evaluations could, for the most part, be accomplished without the subsystem level NTR configuration being completely identified. The results of this analysis is given in Figure 4-11.

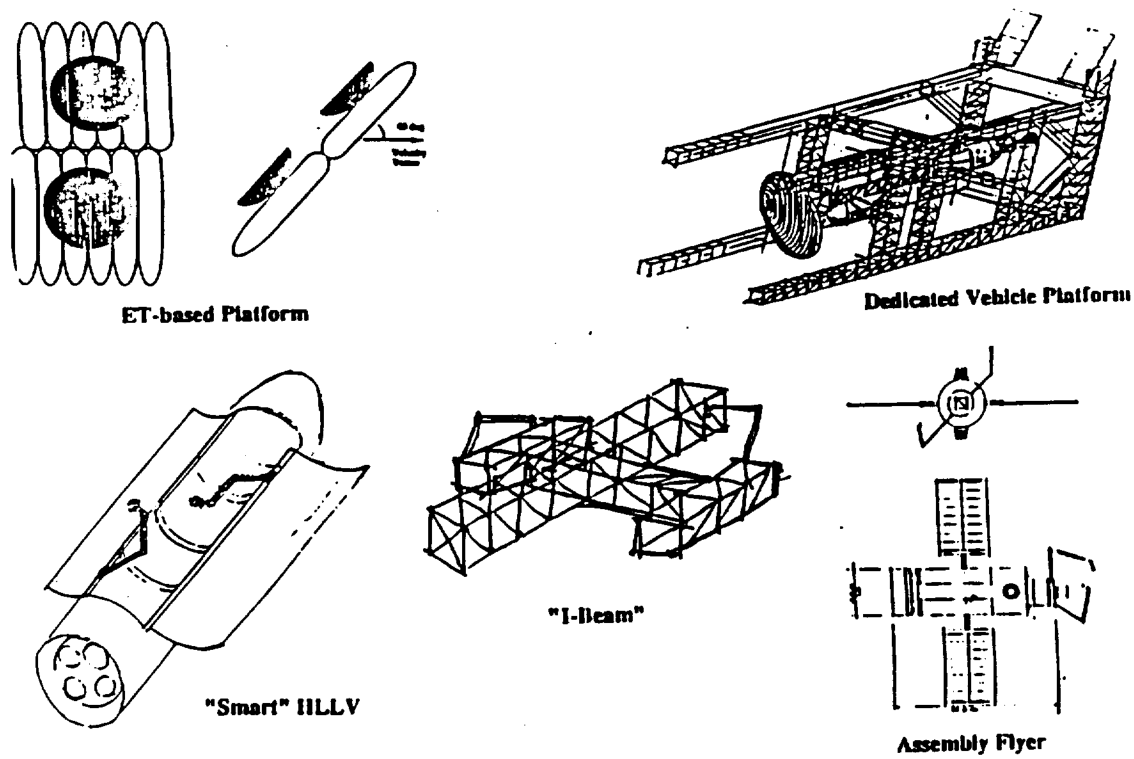

FIGURE 4-1A ON-ORBIT ASSEMBLY CONCEPTS

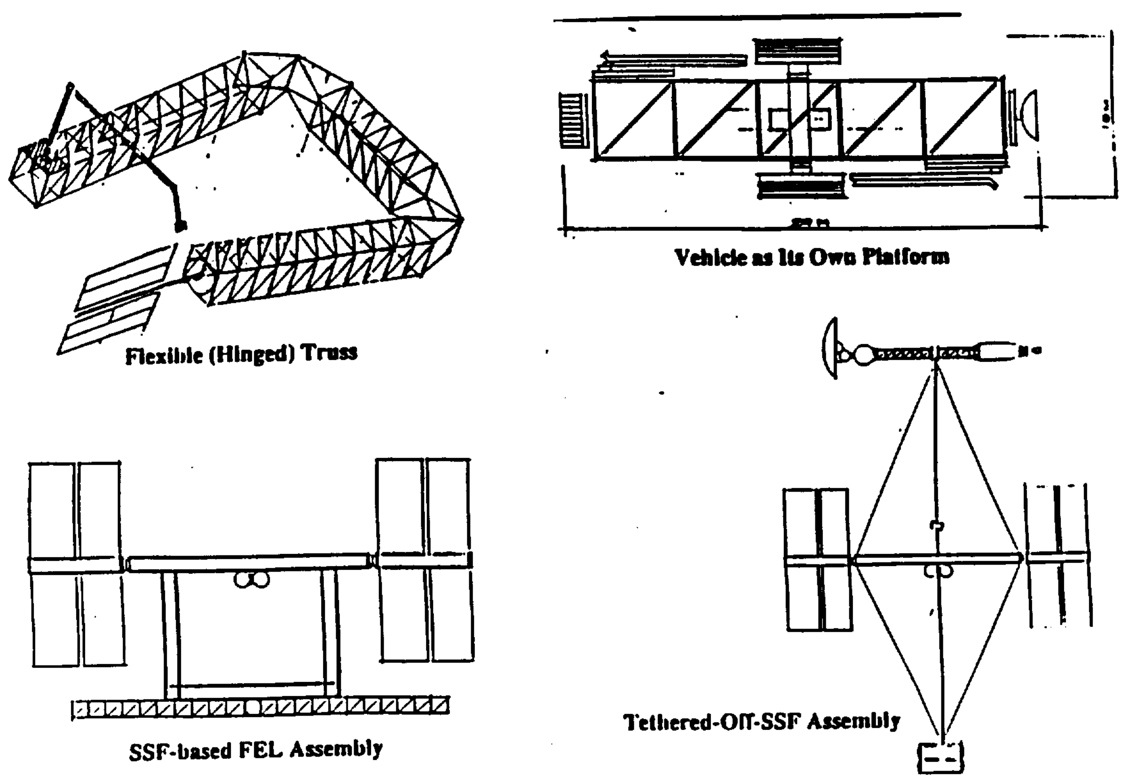

FIGURE 4-1B ON-ORBIT ASSEMBLY CONCEPTS

Node Concepts	Key Features/Advantages	Key Disadvantages
Dedicated Assembly Node	• Abundant storage • Totally self-contained • Vehicle systems unused • Multiple robot arms • Sections of vehicle may be assembled simultaneously	• Larger than SSF • Will take long time to construct • Excessive reboost requirements • Mechanically complex • Local debris shielding required • Must be in place prior to vehicle assembly
I-Beam Platform	• Can be carried up in first HLLV flight • Can easily reach most parts of vehicle with two robot arms • Uses vehicle for comm., data, RCS, power after initial deployment • Can serve as base for experiments	• Fuel cells, batteries required for initial deployment • Limited storage area • Precursor mission required for deployment
"Smart" HLLV Platform	• No additional platform required • HLLV shroud provides limited debris shielding • HLLV provides for communication, data, RCS, GNC, etc. • Robot arms transferable to NTR	• Increased HLLV complexity • Reboost fuel has to be replenished • Limited storage • Vehicle must be detached from HLLV prior to assembly complete • Local debris shielding required
Hinged Truss Platform	• Uses vehicle truss as assembly platform; no other platform needed • Reach to remote engine section of vehicle provided by flexing truss at hinges • Vehicle subsystems used; no additional systems necessary	• Requires a precursor mission to deploy truss • Batteries, fuel cells necessary for initial deployment • Reboost, comm., data, power, must be in place prior to assembly start • Limited storage • Local debris shielding required
Vehicle as its own Platform	• Reduces needed on-orbit infrastructure • Deletes additional facilities and resources needed for designing, builiding, launching, and maintaining separate assembly platform	• Requires dedicated HLLV flight for non-optimized packaged first element • Requires vehicle to have additional control, reboost • No additional storage • Requires batteries or fuel cells for initial deployment • Requires localized debris shielding

Node Concepts	Key Features/Advantages	Key Disadvantages
Assembly Flyer Platform	• Performs HLLV unloading, payload/crew transport, and assembly with one vehicle • Compatible with SSF • Capable of manned/robotic operations • Uses CTV for main P/A • Can serve as free flying platform between assemblies	• No additional storage • Requires vehicle to have additional control and reboost systems • Requires development and production of sophisticated man-rated space vehicle • Requires localized debris shielding
SSF Based Assembly of First Element	• Uses planned SSF growth concept • Provides quick and easy crew logistics access to initial assembly operations • Allows verification and checkout of critical systems prior to independent vehicle operations • Does not disrupt SSF operations beyond first assembly mission (remainder of assembly based from vehicle itself)	• Impact to SSF (resources, microgravity, drag, etc.) • Eventually requires vehicle to have additional control and reboost systems • Requires localized debris shielding • No additional storage beyond first element
Tethered off-SSF Assembly Platform	• Compatible with current SSF design • Provides quick and easy crew and logistics access to entire assembly and propellant transfer operations • Microgravity and dynamic loads impacts to SSF minimized by tether • Removes hazardous operations and materials to SSF standoff distance	• Impact to SSF resources • Requires localized debris shielding • No additional storage • Requires additional reboost and control systems on SSF

FIGURE 4-2 ASSEMBLY NODE CONCEPTS PROS AND CONS

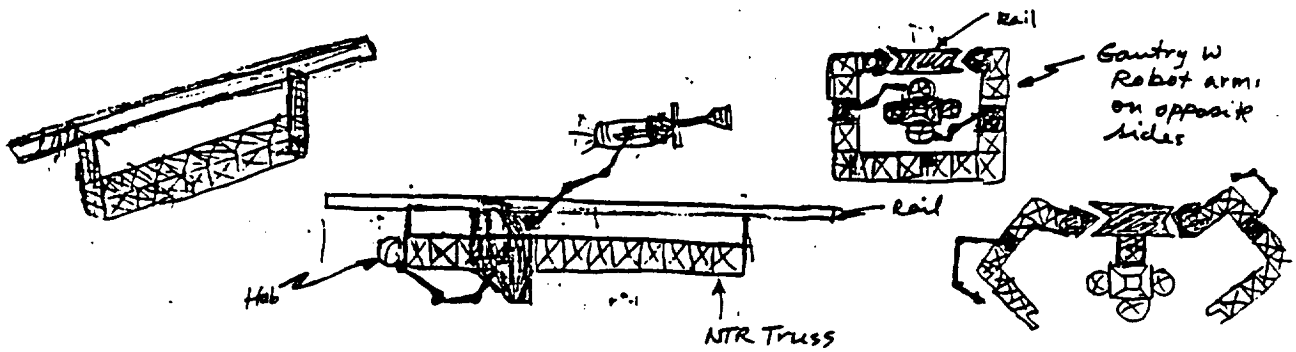

FIGURE 4-3 ON-ORBIT ASSEMBLY CONCEPTS

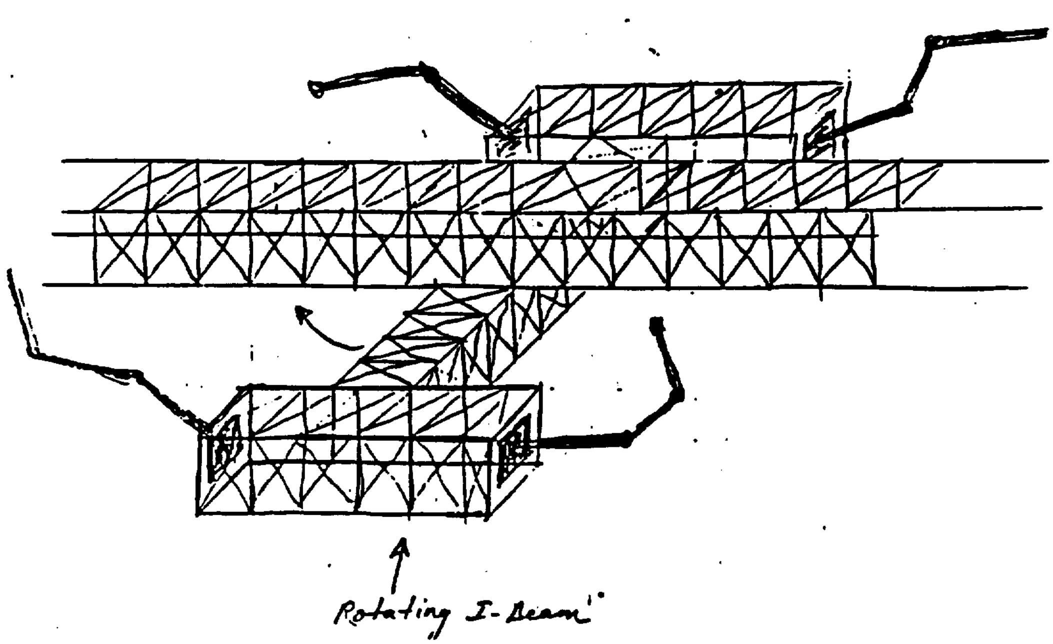

FIGURE 4-4 MODIFIED I-BEAM WITH LAZY SUSAN

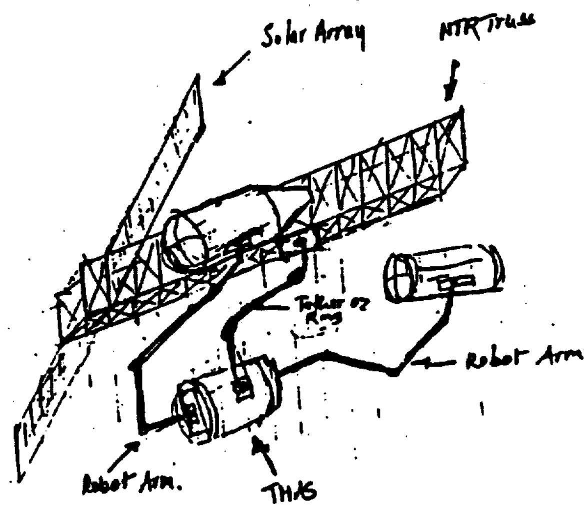

FIGURE 4-5 COMMON HAD AND ASSEMBLER/SERVICER

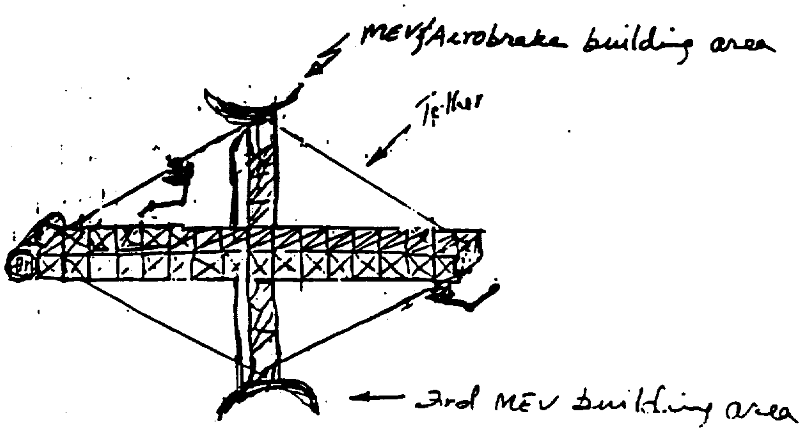

FIGURE 4-6 TETHERED ROBOTIC ASSEMBLY PLATFORM

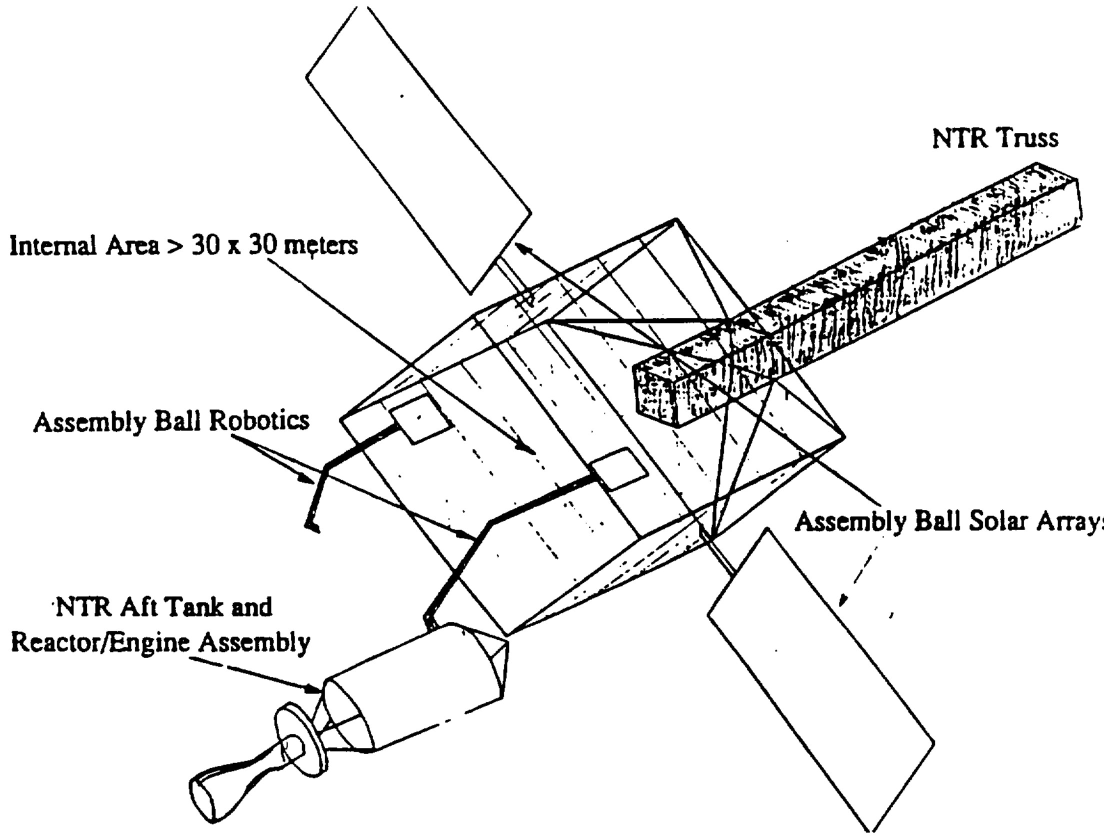

FIGURE 4-7 ASSEMBLY BALL PLATFORM CONCEPT

Major Features	Major Concerns
• Provides 360° of access to particular assembly area • Multi-faceted (square, pentagon, hexagon, etc.) structure: - Partially deployed (solar arrays, booms, etc.) - Partially constructed (via STS, SSF, CTV, etc.) - May be easily disassembled once NTR complete • Fully self-supporting and/or synergetic with NTR - NTR robotics may be used to attach tanks - Power, TCS, etc. may be to or from NTR - Transportable along NTR truss • Sized to envelope Aeroshell for its assembly • External faces allow systems attachment (solar arrays, antennas, etc.) and some storage • Operates with one or both "ends" closed	• Limited storage capacity • Limited compatibility with pressurized assembly modules • Reboost and control system location (NTR itself, separat vehicle, etc.) • Platform requires some assembly of its own • May not be as compatible with multi-lander NTR, NEP, SEP • Refurbishment operations: - Capture of returning NTR - Nuclear reactor related tasks • Resupply issues • Localized shielding for NTR and platform required

FIGURE 4-8 ASSEMBLY BALL PLATFORM CONCEPT - FEATURES AND CONCERNS

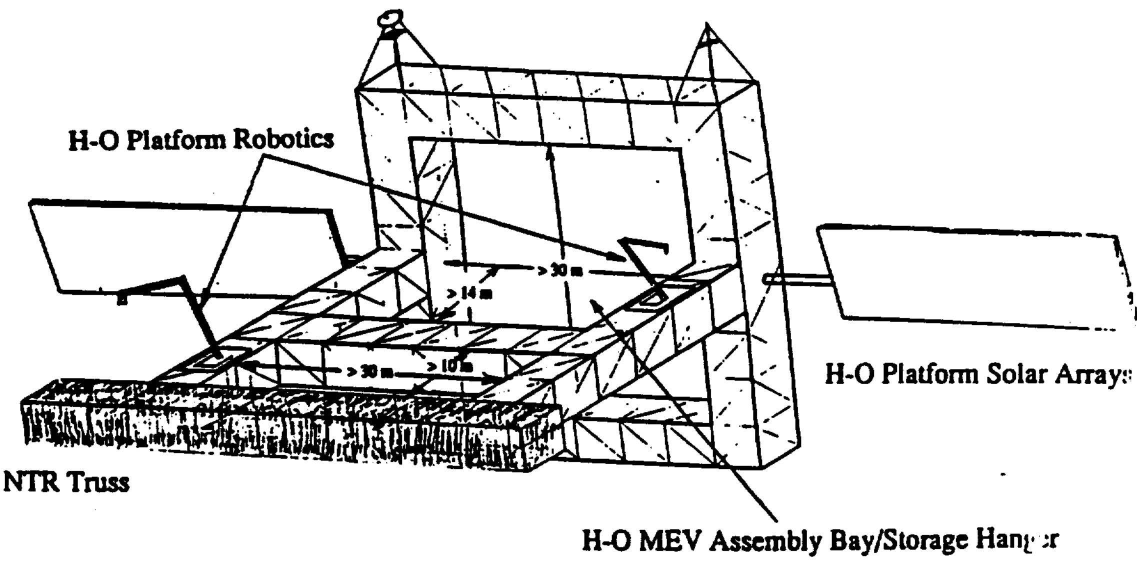

FIGURE 4-9 H-O ASSEMBLY PLATFORM CONCEPT

Major Features	Major Concerns
• Expansion of "I-Beam" platform concept • Fully self-supporting with possible synergism with NTR - NTR robotics may be used to attach aft tank or transfer MEV to NTR - Power, TCS, etc. may be to NTR - Transportable along NTR truss • Allows separate and parallel MEV and NTR assembly • Similar to SSF planned growth configuration • MEV assembly bay doubles as storage hanger • Man-tended/permanent modules easily added • May be compatible with NEP, SEP, and (with addition of second bay) CAB • May serve as experiment station between assembly activities	• Nearly as large and complex as SSF • Requires significant assembly of its own • Localized shielding for NTR and platform required • Additional structure may be required to accommodate CTV, STV, STS, etc. docking • Controllability of full/near-complete NTR • Maneuvering MEV to NTR (may allow test of MEV/NTR rendezvous and docking, MEV propulsion, etc.) • Resupply issues

FIGURE 4-10 H-O ASSEMBLY PLATFORM CONCEPT - FEATURES AND CONCERNS

Concepts	Accept	TBD	Reject	Rationale
Free- Flying Concepts: Dedicated Platform			√	requires too many launches, too high a level of support, and will be too time consuming to construct on orbit
I- Beam plain modified "lazy susan"	√			this class of platforms appears to fulfill the buildup requirements
Smart HLLV	will not be used alone, but will be evaluated for use with other platforms			
Vehicle as the Platform		√		requires a better definition of the vehicle configuration
Assembly Flyer	will not be used alone, but will be evaluated for use with other platforms			
Tethered Robotic Assembly			√	length of central beam prohibitively long for the robots to clear the tanks
Gantry on Rail	√			this class of platforms appears to fulfill the buildup requirements
Common Hab and Assembly/Servicer	√			this class of platforms appears to fulfill the buildup requirements
Assembly Ball Platform		√		possible interference with major components
H-O Assembly Platform			√	same as the Dedicated Platform
Hinged Truss			√	this configuration has too many complications for use with this type of vehicle
Attached to SSF: SSF- FEL Assembly		√		1) current design of SSF may not allow extended truss structures or tethered platforms to be attached to the basic structure
Tethered off SSF Assembly				2) the impact to SSF schedules, buildup and function are not yet determined

Accept: will be given first consideration in the analysis
TBD: requires more information to evaluate
Reject: eliminated from consideration

FIGURE 4-11 PRELIMINARY NTR PLATFORM ASSESSMENT

5. CREW MODULES

The Earth Crew Capture Vehicle (ECCV), as configured early in the Phase 1 study, was designed to return four crew to Space Station Freedom following a Mars mission. The present vehicle has evolved into a direct entry capsule for a crew of six, and is also being considered for returning four crew from an early Lunar mission. As the evolved ECCV does not capture, but returns direct to Earth, a more appropriate acronym for the vehicle might be the Crew Return Vehicle (CRV). Assumptions and mission modes for both the Lunar and Mars cases are shown in Figure 5.1.

There are currently several studies underway for design of an Assured Crew Return Vehicle (ACRV) for use at Space Station Freedom, and of a Personnel Launch System (PLS) that would ferry crew to and from space station using an expendable launch vehicle, such as the Titan Four. Both of these systems are currently being designed as short duration (1-10 day) crew modules, and therefore have some commonality with the CRV.

Sources of data for configuration of the CRV, and sizing of it's subsystems, are the Boeing PLS, Apollo CM and NASA Langley CERV. The NASA standard 3000 is used as an aid in developing efficient and habitable crew volumes. The reference 6 crew CRV is illustrated in three orthagonal views in Figure 5.2. The Lunar version of the vehicle would be configured with only 4 crew couches.

During this study, questions arose concerning the need for a higher L/D, and greater crossrange for the CRV. A decision was made to briefly study a possible configuration that would satisfy both Lunar and Mars mission modes, and also offer higher crossrange capability, lower g loads on entry, and greater landing site availability. The preliminary configuration for the high L/D CRV is shown in Figure 5.3.

The high L/D CRV is assumed to fly at a relative wind angle that would produce an L/D of aproximately 1.0, and would utilize a parachute or parafoil system for final descent and landing. Further work on this task will include trajectory and heating analysis for both the reference and high L/D configurations, estimation of g loads on the crew during entry, and investigation of "dry" landing systems. There will also be continued work on structural and heat protection systems that will have a positive impact on the mass of the vehicle.

Assumptions

- Direct entry CRV need not be common with SSF ACRV due to higher entry velocity
- Tanden Direct Lunar missions will be limited in number, making reusability a lower priority.
- CRV payload mass is relatively low(crew, surface samples and data), allowing parachute or parafoil landing.
- CRV propulsion limited to ACS
- LTV provides power prior to earth entry

Mission Modes

- 10 day nominal duration for 4 crew.
- 30 days on Lunar surface in "powered down" mode without crew.
- Separation from LTV 24 hours or less prior to direct Earth entry.
- Parachute or parafoil descent and "dry" landing.

FIGURE 5-1A LUNAR CRV, ASSUMPTIONS AND MISSION MODES

Assumptions

- Direct entry CRV need not be common with SSF ACRV due to higher entry velocity
- Direct entry missions will be limited in number, making reusability a lower priority.
- CRV payload mass is relatively low(crew, surface samples and data), allowing parachute or parafoil landing.
- CRV propulsion limited to ACS
- MTV provides power prior to earth entry

Mission Modes

- 24 hour duration for 6 crew.
- Up to 1000 days attached to MTV in "powered down" mode
- Separation from MTV 24 hours or less prior to direct Earth entry.
- Parachute or parafoil descent and "dry" landing.

FIGURE 5-1B MARS CRV, ASSUMPTIONS AND MISSION MODES

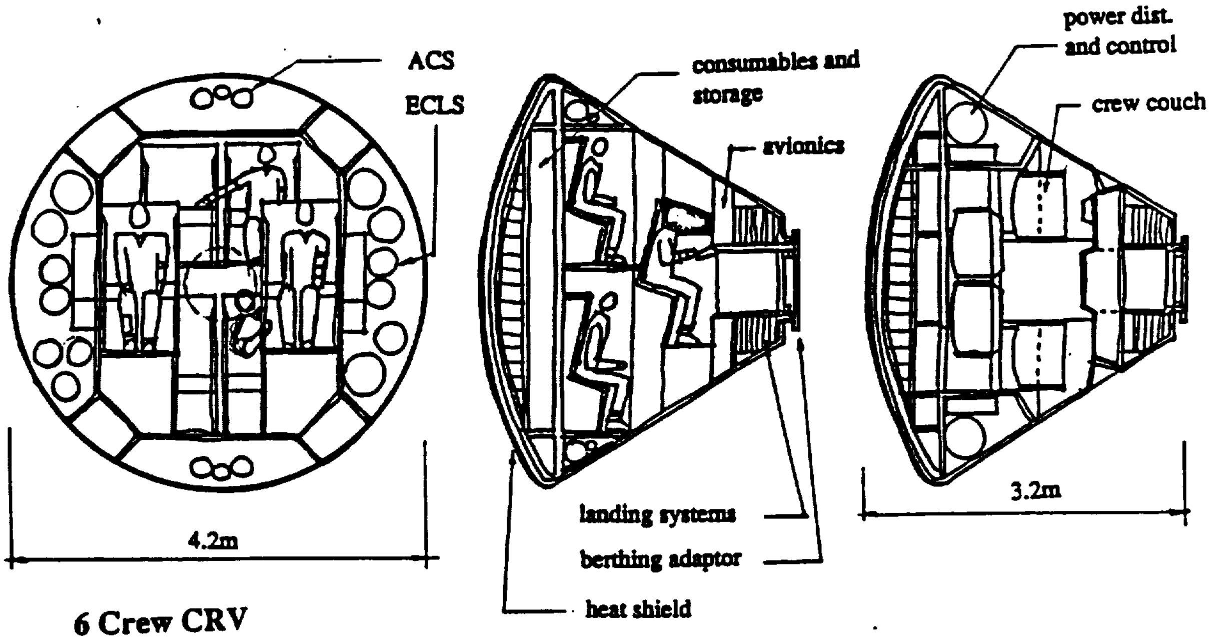

FIGURE 5-2 CRV CONFIGURATIONS

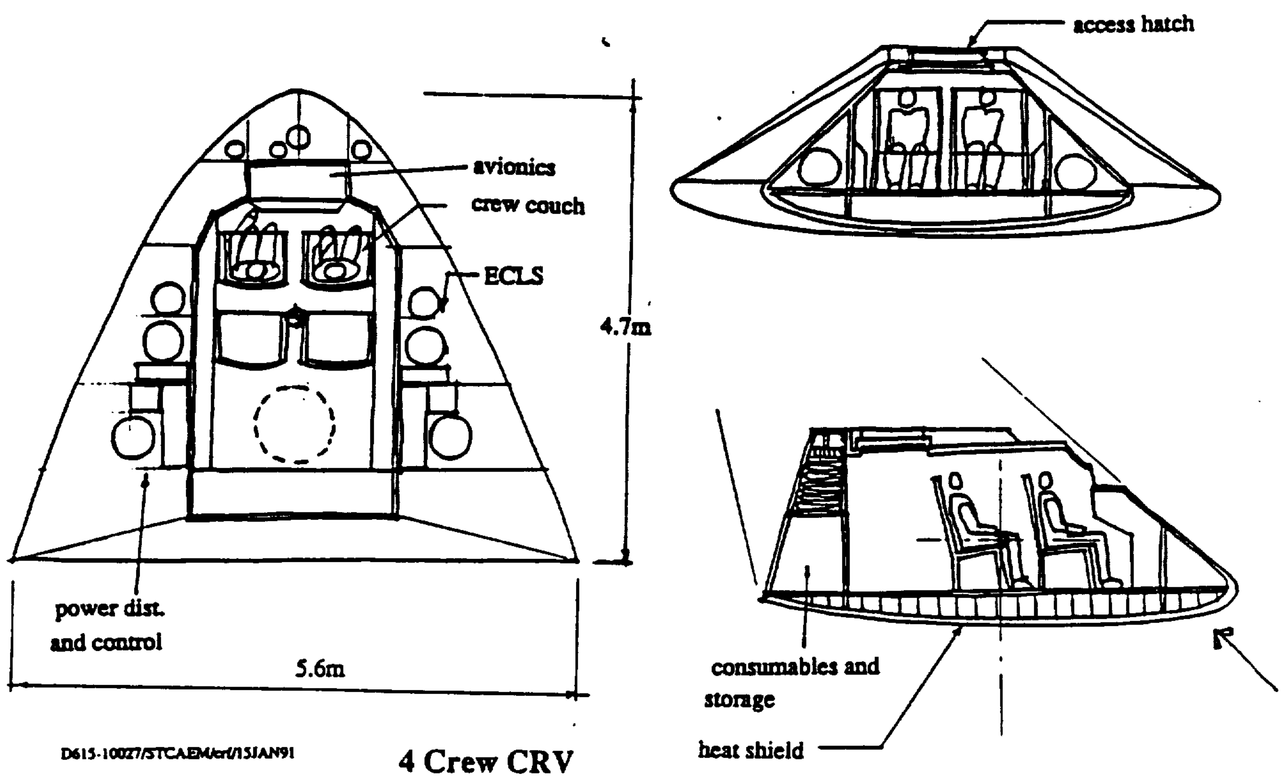

FIGURE 5-3 HIGH L/D CRV CONFIGURATIONS

6.0 FLIGHT DYNAMICS

Modifications to the Boeing PLANET code were underway for the duration of TD5. These modifications were concerned with one way contours with embedded deep space maneuvers (DSM). Work has proceeded well and preliminary C3L and total delta-V contours have been generated for a few test dates. C3L is defined as the square of the departure hyperbolic excess velocity. Verification of the accuracy of this contour generating routine is now being performed through comparisons with DSM data provided by Marshall Space Flight Center and the Jet Propulsion Laboratories.

A C3L contour for the 2025 opportunity is shown in Figure 6-1. This contour is a typical 1-way Earth-to-Mars contour with no DSM's simulated during the transfer. Note that for this region of mission space the C3L values are relatively large with values on the order of 200 km^2/s^2. A C3L contour for the identical 2025 opportunity, but with embedded DSM's simulated for the transfer is shown in Figure 6-2. A comparison of C3L values from these two figures indicates a significant and general decrease in launch energy requirements over direct transfers through utilizing DSM's. As a specific example, a comparison is made of C3L values for the Julian launch date of 2460330. For this launch date, the minimum C3L value shown in the direct transfer contour is approximately 220 km^2/s^2; a minimum C3L of approximately 45 km^2/s^2 is shown in the DSM contour. This difference in C3L translates into a departure delta-V difference of about 5.7 km/s for a space station type circular orbital altitude of 500 km. Also, it can be seen for the 2460330 launch date that the DSM minimum C3L value has been shifted ahead by some 30 days. An explanation of this arrival date shift is found in realizing that for a particular launch date a DSM trajectory will be a longer and a lower energy trajectory, thus an intuitively later arrival date is expected.

Some examples of launch-date/arrival-date have been found for which the PLANET DSM search routine will not find a true minimum energy trajectory. This problem is thought to be related to certain high energy "ridge" related anomalies. A simple ridge-countermeasure algorithm has been implemented for general ridge related trajectories, but for these aforementioned anomalies, a modification of the search routine must be made to increase the initial mid-point radius vector used as an initial guess for the DSM location.

Further PLANET modifications will be made allowing for the generation of round trip contours with embedded DSM's. This round trip procedure will search the prescribed mission space for potential DSM's for the outbound and inbound legs of the trajectory.

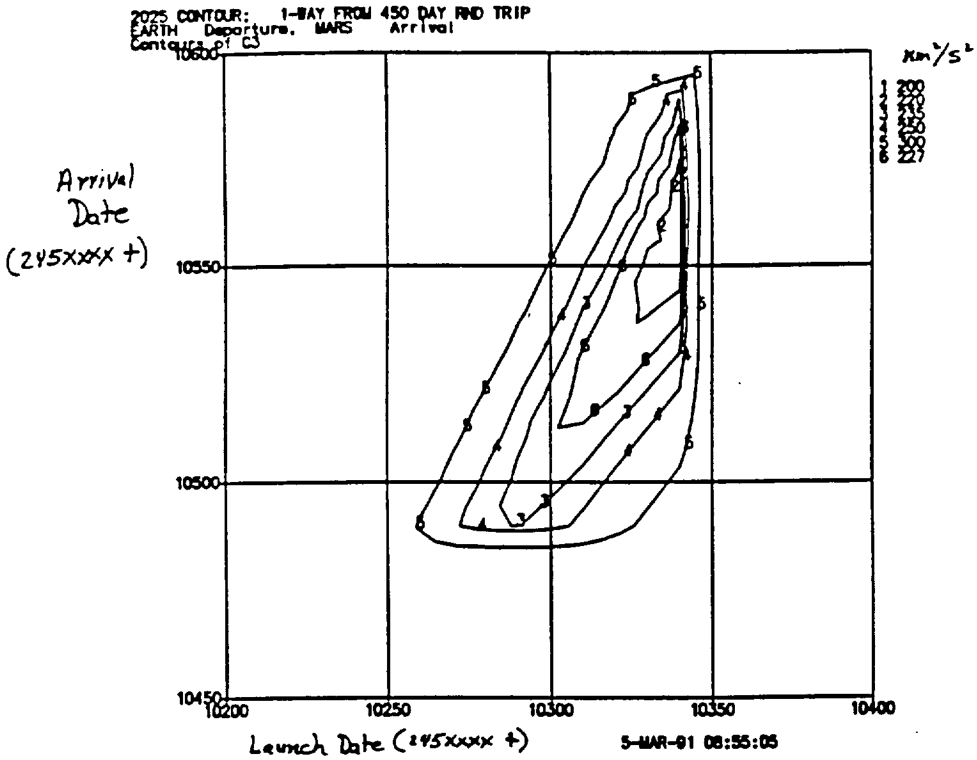

FIGURE 6-1 C3L CONTOUR WITHOUT DEEP SPACE MANEUVERS

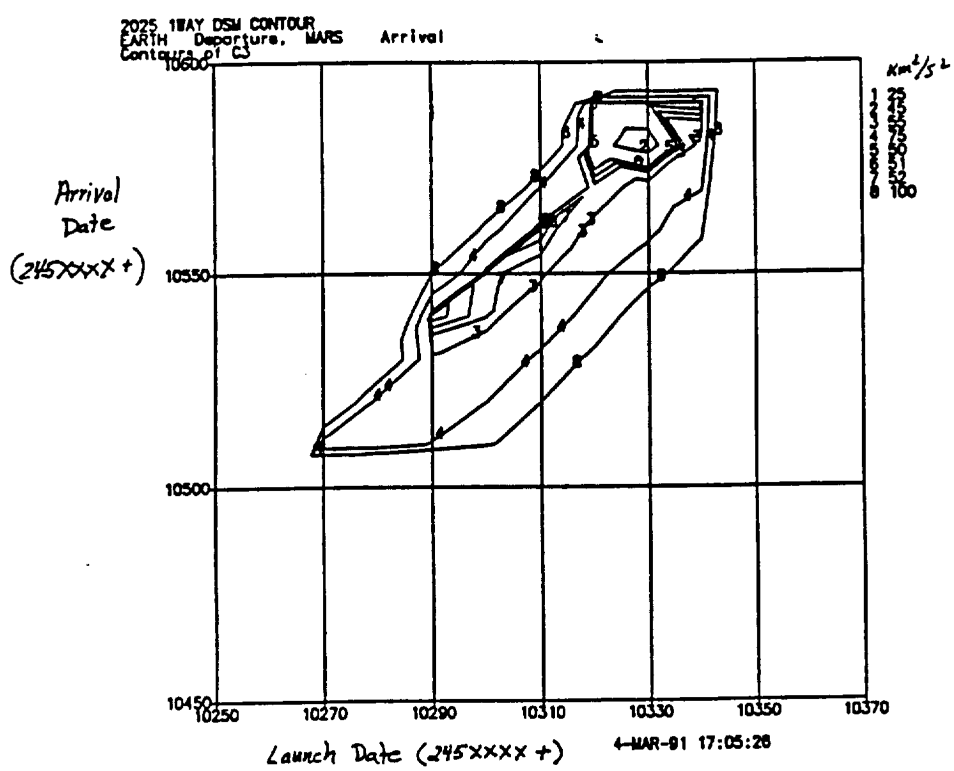

FIGURE 6-2 C3L CONTOUR WITH EMBEDDED DEEP SPACE MANEUVERS

7. ARCHITECTURE ASSESSMENT, PROGRAMMATICS ANALYSIS, AND TECHNOLOGY ADVANCEMENT

Several activities were conducted in these areas. A brief discussion on the topics examined are provided. A presentation was made on "Power Beaming". The presentation material is provided in Appendix A.

7.1 Beam Power Electric Orbit Transfer Vehicle

7.1.1 The Case for Power Beaming

Frequently mentioned as power sources for electric propulsion are nuclear and solar electric generators. Power beaming is a third option, one which removes much of the power generation mass from the vehicle, offering the potential for greatly improved performance. It is possible to beam power by charged particles, neutral particles, or electromagnetic waves. Practical means of converting particle beams to useful electric power at the receiver are not at hand, leaving electromagnetic waves, either microwaves or laser beams, as candidates for beaming power to transportation vehicles.

7.1.2 Microwave vs. Laser

Microwave power beaming received considerable study and technology attention during several solar power satellite (SPS) studies from 1968 through 1981. SPS design studies considered beaming as much as 5000 megawatts net delivered electric power from large satellites in geosynchronous orbit to receiving stations on Earth. Laboratory tests demonstrated more than 50% end-to-end (electrical to electrical) efficiency. An experiment at the JPL Goldstone station demonstrated efficient receiving of more than 30 kWe electric power from a high-power transmitter (the entire transmitted lobe was not intercepted by the receiver). A Canadian experiment demonstrated continuous powered flight of a microwave-powered model airplane. The airplane carried a lightweight microwave power receiver; its propeller was driven by the resulting electric power. The main argument for microwave transmission is efficient power transfer. The main argument against microwave power transmission is large aperture products at long distances, i.e. very large phased-array antennas are necessary.

High-power lasers have been developed in weapons research, mainly SDI but also as potential battlefield weapons. Experimental lasers have destroyed targets in flight. Experiments have demonstrated principles of adaptive optics for high beam quality. Power transfer experiments have demonstrated coupling of laser energy through windows to gas flowing in a laser "combustion" chamber, and to solar cells. Laboratory tests have shown greater than 50% efficiency in converting laser light to electricity. High efficiency results because the monochromatic laser light is matched to the solar cell band gap. Much of the broad-spectrum sunlight received by a solar cell is not well matched and either is converted inefficiently or not at all.

Lasers suitable for power beaming to space vehicles will probably be of the electric-to-laser energy type. There are two principal candidates, free-electron lasers and solid-state quantum-well devices. The latter offer higher efficiency but are small devices; very large numbers would have to be phase-locked in an array. A free-electron laser converts energy in a high-power electron beam to laser light. The power from a single device is limited only by the power in the electron beam and by the power capability of the optics. End-to-end efficiency estimates range from about 5% to about 20%, compared to 50% demonstrated and projections as high as 70% for microwaves.

If the power beam source is on Earth, the lower efficiencies in the laser range are not of primary concern. For example, an EOTV mission to the Moon might use 10 megawatts electric power for 4000 hours. At 5% efficiency and 5 cents/kWh, the cost of power is $40 million. The high propulsive efficiency of a power-beam EOTV would save at least one HLV flight worth at least $200 million.

Laser power beaming also reduces concern for solar array cost. Trades performed on this study indicated that solar array cost is a major issue for solar-electric propulsion systems and that present-day costs (~$1000/watt) are about a factor of ten too high for economic electric propulsion service. Laser power beaming addresses this issue by increasing the power delivered per unit array area by about a factor of ten, e.g. four suns' intensity and more than twice the array efficiency.

7.1.3 Inclined Orbits

Analyses of power beaming to electric orbit transfer vehicles by Raytheon have proposed equatorial beaming sites and equatorial orbits for maximum power beam availability to the

EOTV. This, however, precludes U. S. space operations from U. S. launch sites, e.g. KSC. A most conservative view would constrain the EOTV starting orbit to 28.5 degree inclination and power beaming sites to U. S. locations (Hawaii included). In the case of inclined orbits, it is better to place the power beam sites at latitudes close to the orbit inclination for maximum power beam availability.

7.1.4 Beam EOTV Simulator

A beam-power EOTV simulator has been developed to answer the key questions associated with inclined orbit operations. These questions are stated in Figure 7-1. The features of the simulator are summarized in Figure 7-2.

7.1.5 The "Unwrap" Condition

Boeing space transportation studies performed many years ago determined that there is a critical acceleration level at which the low-thrust spiral about a central body "unwraps" to an escape trajectory, and that this critical acceleration level is about 1/(2*pi) times the local gravitational acceleration of the central body. At this level, the energy added to the orbit in one revolution is equal to the energy needed for escape. Available acceleration is related to power-to-mass ratio and Isp. The following table gives typical power-to-mass ratios in kg/kWe for "unwrap" acceleration at typical distances from the Earth:

Isp	1500 sec	10,000 sec
Radius		
10,000	0.2	0.03
50,000	5.0 0	.75
100,000	20.0	3.0
200,000	80.0	12.0

LEO radius is about 6800 km. GEO radius is about 40,000 km. Lunar radius is about 400,000 km. 1500 seconds is a typical arcjet Isp; 10,000 is typical for ion thrusters. A typical beam power EOTV system would be at 5 to 10 kg/kWe, including propellant and payload. These "unwrap" conditions apply for continuous power availability.

7.1.6 Initial Simulation Results

We conducted an initial beam power EOTV simulation to get an idea of the power-on duty cycle for only continental U. S. sites, and to address the question whether sites concentrated in one geographical locale would lead to highly elliptic orbits due to "periapsis pulsing". Results are shown in Figures 7-3 and 7-4. An acceptable rate of orbit raising was achieved. The turn-over of eccentricity indicates that Earth rotation effects and secular advance of the line of apsides prevents excessive ellipticity of the transfer orbit. We will continue EOTV simulations to better determine lunar transfer performance.

7.2 Earth Orbit Return From Mars Transfer

7.2.1 Return Geometry

Return to a particular low Earth orbit such as the Space Station Freedom orbit is constrained to the times when the orbit contains the return S-vector. If the S-vector declination is less than the inclination of the Space Station orbit, there will be two particular orbit line of nodes cases where the orbit contains the S-vector. If the S-vector declination is greater, the Space Station orbit cannot contain the S-vector and a plane change is necessary upon Earth return. Since the Space Station line of nodes regresses at about 7 degrees per day, there are two times within a roughly 52-day period when return conditions are right. This is a very onerous constraint on Mars mission design, since trajectory times need to be selected to minimize transfer energies. Consequently, we have adopted a phased return strategy that brings the crew directly to Earth in a crew recovery vehicle (CRV) and uses a phasing orbit for Mars transfer vehicle return.

7.2.2 Recovery Scenario

This recovery strategy is depicted in Figure 7-5. The crew returns directly to Earth via the CRV, or deorbits from the elliptic capture orbit immediately after capture. The vehicle is captured in a highly elliptic orbit such as the one depicted with a 24-hour period. The capture orbit is at 28.5 degree inclination for eventual compatibility with the Space Station orbit. One of two capture orbits can be selected; ordinarily we would select the one with the least wait period. After the wait, the line of nodes of the capture orbit is the same as for the Space Station orbit. At that time, an LTV is dispatched to the vehicle to refuel it for an orbit-lowering burn. The NTP vehicle, for example, needs about 30 t. of hydrogen to return it to LEO. It is much more efficient to refuel than for the NTP vehicle to carry the orbit-lowering propellant on the Mars mission.

7.3 Alternate Lunar Mission

7.3.1 Campsite

Capability for an early lunar man-tended surface mission is described elsewhere in this report under the "campsite" task. The campsite investigation concluded that a turn-key overnight lunar habitat could be built for 20 t. total cargo mass. It is desired to deliver this to the Moon on a single HLV flight. This requirement somewhat exceeds the nominal performance of an HLV using 2 ASRMs and a 4-SSME core stage. Estimated delivery capability as a function of mass to translunar injection (TLI) and Isp of the lunar cargo vehicle is shown in Figure 7-6. Based on this figure, we targeted a launcher performance capability of 50 t. TLI.

7.3.2 Crew Mission

A modest crew mission can be accomplished at the 50 t. TLI level. Our preliminary estimates are: 4-person crew return vehicle (CRV) at 5.5 t., support equipment (power & consumables) for the CRV in the lunar stage at 1 t., delivered cargo 2 t., and return science payload including packaging 0.5 t. This leads to approximately 47 t. TLI requirement. About 1 t. of the delivered cargo is needed to resupply the campsite with consumables.

The mission mode is direct expendable with only the CRV returned to Earth. There are no parking orbit or lunar orbit constraints; the mission can go anywhere on the visible lunar surface any time and return any time. Since the crew time in the CRV is only 3 days each way, no additional transfer crew volume is required. The crew spends lunar surface time in the campsite, which includes a solar flare storm shelter.

7.3.3 Launcher Concept

Parametric scaling equations indicate that a launch vehicle with 2 ASRMs, 4 SSMEs, standard ET capacity, and a third stage with about 200 t. propellant load and one SSME can deliver 50 t. to TLI. This of course requires modification of the SSME for air start; two starts are required.

The performance gain arises from significant reduction in effective mass delivered to orbit since the third stage starts at roughly 3000 m/sec less than orbital velocity.

If this scheme works, it provides an initial manned lunar capability with a minimum of development projects: CRV, lunar stage, and campsite module, science payloads, and the HLV third stage if it is not accounted to the HLV program. No orbital operations or nodes are needed. The lunar vehicle is in the LEV class, and could become the LEV for permanent lunar base operations.

7.3.4 Science Candidates

Although this mission capability is modest, it is large compared to Apollo and could support significant science, including (1) an early technology demonstrator for a lunar optical interferometer, (2) unpressurized rovers for lunar geoscience, and (3) small-scale in-situ materials use (ISMU) experiments. In addition, the campsite cargo delivery capability of 20 t. could be used to deliver large science and surface operations systems.

7.4 Power Beaming Presentation

During the month of February, effort was spent on the power beaming portion of the programmatics task. Brad Cothran and Brent Sherwood were invited to give a presentation at Lewis Research Center for a power beaming kick-off meeting. The focus of the meeting was technology for a future power beaming program. John Rather of NASA headquarters was the meeting chairman. New charts from this presentation are provided in Appmdix A; backup charts (surface system designs and analyses from an earlier Boeing study for Ames Research Center, NAS2-12108) are not included.

After the meeting we were asked by Whitt Brantley of MSFC to assist him in a power beaming presentation to be given at headquarters at the first of March. Some charts were generated and are also included in the attachments. The effort expended on power beaming is directed an Earth based power beam transmitter to an Electric Orbital Transfer Vehicle and power for a Lunar Base. Computer Simulations necessary to generate data for the EOTV analysis are being finalized. Technology inputs for the power beaming system were also obtained from the workshop.

- **Currently an Earth based laser transmission system coupled with an EOTV and or Lunar base, show the most promise for economic return.**
- **How does the performance (trip time and payload) of a power beam EOTV in an inclined orbit vary with number and distribution of ground stations?**
- **Assuming that power transmission to the Moon gets first priority, and considering typical weather and laser plant reliability, what is the beam power availability for the EOTV and how much is it expected to vary?**
- **How does the life cycle cost of a lunar surface/EOTV power beaming system trade with the conventional approach of cryogenic propulsion and nuclear reactors power for the lunar surface.**

FIGURE 7-1 POWER BEAMING: KEY ISSUES AND QUESTIONS - NEAR TERM APPLICATIONS

- **Generates ground track over rotating Earth.**
- **Determines visibility and range from selected ground stations, up to 20 stations. Minimum beam elevation angle is a parameter.**
- **Calculates power transfer based on range, wavelength, apertures, available power and assumed beam quality factor.**
- **Numerically integrates orbit raising by thrust based on available power, input mass, and Isp.**
- **Current orbit state feeds back to above steps for every integration step.**

FIGURE 7-2 BEAM POWER EOTV SIMULATION

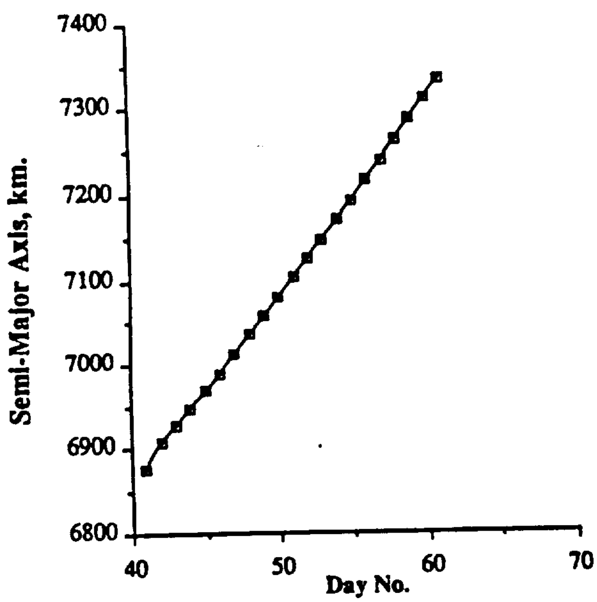

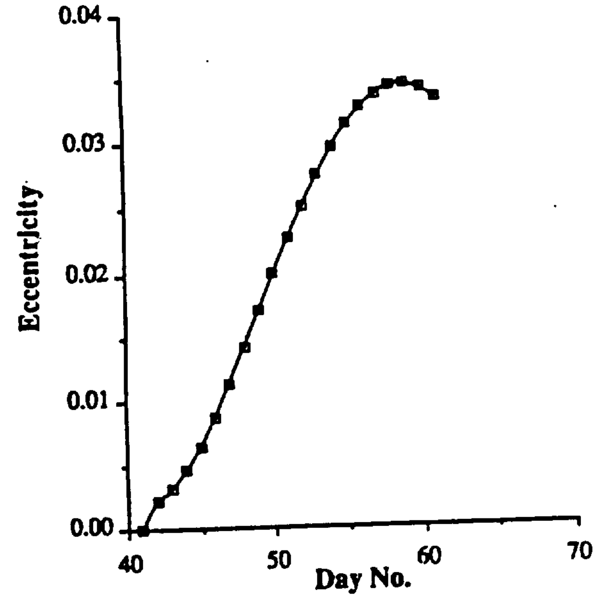

FIGURE 7-3 ORBIT RAISING WITH THREE NORTH AMERICAN SITES

Assumptions

- EOTV total mass 100 t.
- Rated jet power 10 megawatts (means about 15 MW RF power in beam).
- Rated power achieved when EOTV can capture entire main lobe; otherwise power reduced by inverse square law.
- 5000 seconds Isp
- Ground sites at KSC, Brownsville Texas, and Baja Calif.
- Transmitter apertures 100 m except KSC 150 m.
- EOTV aperture 250 m.
- Beams steerable 2 axes down to 30° above horizon.

Results

- Orbit raising performance seems acceptable for as few as 3 ground stations.
- Even at 35 GHz, significant power loss due to beam spreading occurs above 7000 km SMA (about 625 km altitude).
- Orbit eccentricity does not grow without limit.
- This is a "linear" problem, i.e. 1/2 the Isp, 1/2 the time; 1/2 the power-to-weight, twice the time, etc.

FIGURE 7-4 POWER BEAMING SIMULATION ASSUMPTIONS/RESULTS

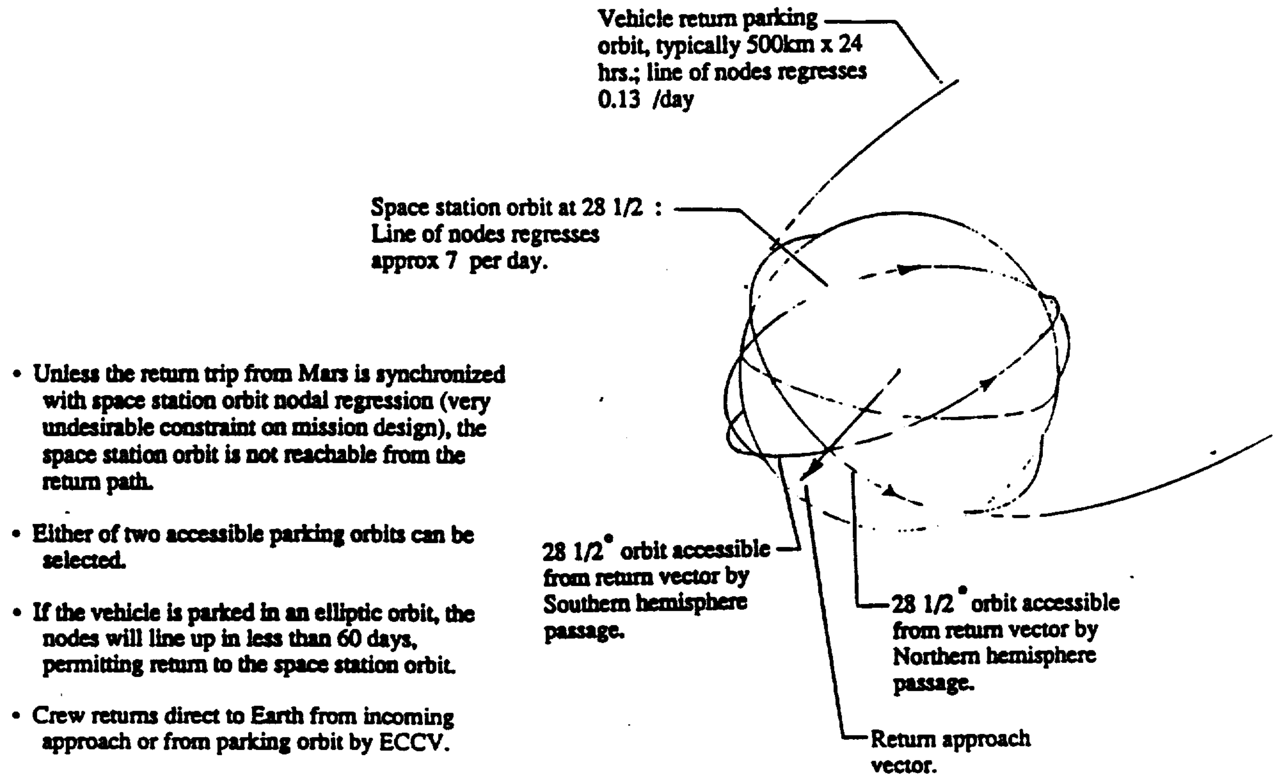

FIGURE 7-5 ECCV RECOMMENDED FOR CREW EARTH RETURN FROM MARS

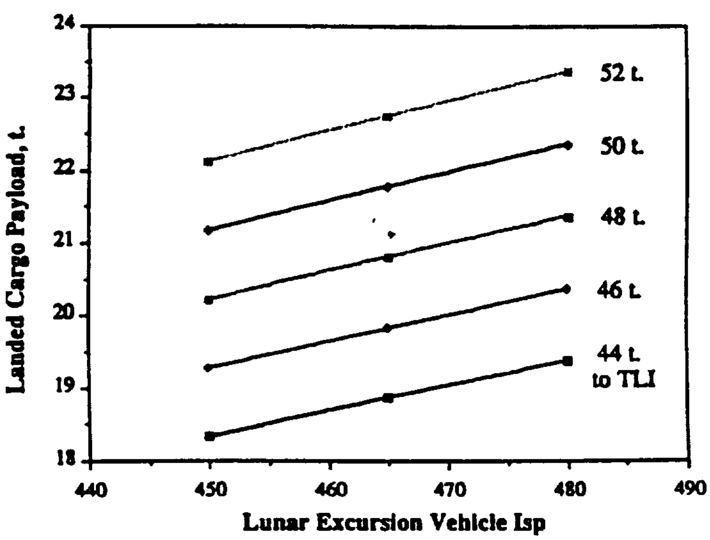

FIGURE 7-6 LUNAR CARGO DELIVERY ESTIMATE

8. SUPPORT TO MSFC SEI ACTIVITIES

8.1 Minimum-Sized Lunar Campsite Analysis

The campsite is a concept which allows early manned missions to the Lunar surface with minimal infrastructure required. The purpose of this task was to do a detailed analysis of the campsite and its support systems to get a preliminary mass statement. A baseline campsite mission was defined for 30 days with a crew of four. Lowest mass options for the Environmental Control and Life Support System (ECLSS) and the External Power System were non-regenerative systems which require resupply for each mission. The analysis included the following systems: Structures, Crew Systems, ECLSS, Internal Electrical Power System, Internal Thermal Control System(TCS), DMS/Communications, Internal Audio & Video, External TCS, External Power System, Science, and Storm Shelter.

The results of this task are summarized in Figure 8.1 and show that a minimum campsite for 30 days with a crew of four will weigh about 20 metric tons. Power, mass, and volume numbers were generated for each system and sources of information are sited. Backup material for each system is included in Appendix B. There is a reasonable degree of confidence in campsite weights for the following reasons:

a. Space Station Freedom PDR data was used for a majority of campsite components.

b. The analysis contains fairly low level detail.

c. A 15% growth margin was included. There are several areas where NASA policy decisions will determine specific requirements (e.g. science, medical facility, and storm shelter). Additional information on potential mass reductions associated with various options (e.g. crew of three, use of composite materials) can also be found in the appendix.

Systems	Mass (kg)	Volume (m^3)	Power (kWe)		Source/Comments
			Cont	Non-CAvg.	
Structures	5,933	106 Module * 7 Airlock	--	0.3	* Total volume which contains internal component volumes
Crew Systems	2,625	58	1.0	0.5	
ECLSS	1,070	5	2.2	0.2	Consumables mass not included.
Internal EPS	495	075	0.4	--	
Internal TCS	405	15	0.03	0.5	
DMS/Communication	545	28	0.9	0.2	
IAV	50	075	--	0.3	
C&T	100	External	0.1	--	
External TCS	1,188	External	(2.2)	--	2.2 kWe during lunar day only.
Power - Open cycle HW	360	External	--	--	Does not include fuel cell reactant mass (1955 kg)
-RFCpack	195	External	--	--	Deployment/Standby power
Science	1,565	8	0.65	1.0	
Storm Shelter	3,465	12	--	--	
15% Growth	1,945	13	--	--	Does not include science or storm shelter approach.
Total	19,940	102	(7.5) 5.3	3.0	

FIGURE 8-1 BASELINE CAMPSITE SUMMARY

APPENDIX A

POWER BEAMING

Power Beaming

Lunar Surface Power Requirements and the SPS Laser Analysis

Brent Sherwood
Brad Cothran

Cleveland, Ohio
February 5, 1991

BOEING

STCAEM/brc/4Feb91/disk10

Laser SPS Analysis

- Major concern of lasers during the SPS analysis was the conversion efficiency of electric to laser was low.

- For ground based power beaming sources, electric to laser efficiency is not a big issue.

- Lasers offered two potential benefits:
  - Transfer smaller blocks of power; broaden market
  - Less environmental concerns

- Lasers were less efficient than microwaves. Proposed substantially improving at least one end of the link.

- Laser technology has advanced since the SPS analysis. Much work is classified.

Study Objectives

SPS Laser Analysis

1. Evaluate and select laser technologies having promise for the SPS power transmission application.

2. Develop candidate SPS system concepts using laser power transmission.

3. Select a "reference" system and provide a comprehensive evaluation.

4. Determine critical issues associated with laser SPS systems and develop a five year ground-based exploratory development plan for key elements of the laser SPS system.

Laser SPS Option Masses

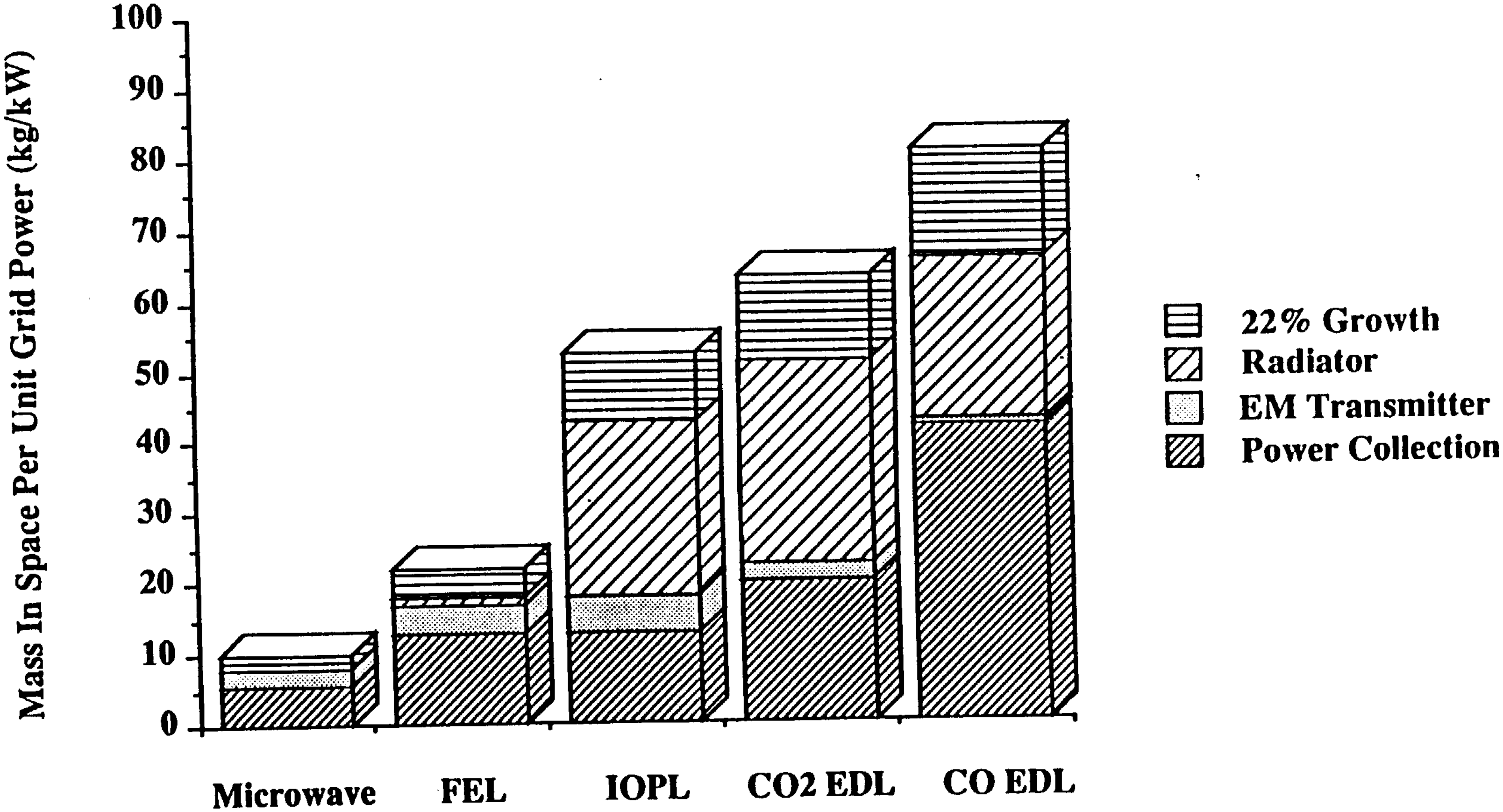

Conclusions

SPS Laser Analysis

- The most promising laser for the SPS application is the FEL.
- The FEL is inherently lighter, scales nicely to commercial utility power levels, and exhibits a distinct advantage in having a tunable wavelength to enhance atmospheric transmission.
- The IOPL was recognized as the second choice.
- Almost all aspects of laser SPS's require technology development.
- Although much analysis was based on future technology, no "can't possibly do's" were identified.

Recommendations

SPS Laser Analysis

In order for establish technical feasibility of the laser alternative to SPS, recommendations in the following areas for a ground based exploratory development program were made:

- Electron Discharge Lasers
- Indirect Optically Pumped Lasers
- Free Electron Laser
- Optical beam control for all lasers
- Laser power receivers

ADVANCED CIVIL SPACE SYSTEMS

Summary of Boeing Work Related to *Power Beaming*

BOEING

- Past involvement with the SPS program provided experience and insight into power beaming architectures and system integration (1980).
- Other NASA funded studies analyzed surface systems and their associated power requirements (1988).
- Key participation in NASA Lunar Energy Enterprise Study (1989).
- Current 4 year contract to demonstrate space based laser technology (originally the ground based FEL).
- Current NASA/MSFC study contract includes power beaming task to analyze electric orbit transfer systems.

Power and Lunar Development

Habitation & Science → *Early ISMU* → *Industrialization*

Order of magnitude increase in power demand

Another order of magnitude increase in power demand

- ~ 20 kWe → early human activity
- ~ 100 kWe → continuous human habitation & lunar science
- ~ 1 MWe → early LLOX production, pilot fabrication experiments
- ~ 5 MWe → early fabrication industry production
- ~ 10 - 100 MWe → growth of resource production base (to 90 % ISMU)
- ~ 100 - 500 MWe → development to mature industry
- ~ 500 MWth → subsurface habitation tunnel melting

RLSO Power Requirements

Key Assumptions

- Man-tended base, produces 100 t/yr LLOX
- Hydrogen reduction of ilmenite
- Solar power, daytime batch operation

Key Findings

- 100 t/yr appropriate for reasonable base buildup
- 4.2 kWe/t LLOX actually produced
- Energy "richness" buys process equipment simplicity
- Daytime solar-powered operation feasible but cumbersome

Power Beaming Architecture Matrix

Power Receiving Location

Power Transmission Location	Earth	LEO	MEO	GEO	L1	L2	LLO	Lunar Surface	Mars Orbit	Mars Surface
Earth	• Remote locations	• Satellites • SSF • EOTV	• Satellites • EOTV	• Satellites • EOTV • Station	• EOTV • Staging nodes	• EOTV • Staging nodes	• EOTV • LLO station	• Base • Surface systems		
LEO		• Satellites • SSF								
MEO	• Utility power grid	• Satellites • SSF • EOTV	• Satellites • EOTV	• Satellites • EOTV • Station	• EOTV • Staging nodes	• EOTV • Staging nodes	• EOTV • LLO station	• Base • Surface systems		
GEO	• Utility power grid	• Satellites • SSF • EOTV	• Satellites • EOTV	• Satellites • EOTV	• EOTV • Staging nodes	• EOTV • Staging nodes	• EOTV • LLO station	• Base • Surface systems		
L1		• Satellites • SSF • EOTV	• Satellites • EOTV	• Satellites • EOTV • Station	• EOTV • Staging nodes	• EOTV • Staging nodes	• EOTV • LLO station	• Base • Surface systems		
L2		• Satellites • SSF • EOTV	• Satellites • EOTV	• Satellites • EOTV • Station	• EOTV • Staging nodes	• EOTV • Staging nodes	• EOTV • LLO station	• Base • Surface systems		
LLO								• Base • Surface systems		
Lunar Surface	• Utility power grid	• Satellites • SSF • EOTV	• Satellites • EOTV	• Satellites • EOTV • Station	• EOTV • Staging nodes	• EOTV • Staging nodes	• EOTV • LLO station	• Base to remote surface sys.		
Mars Orbit									•Phobos & Deimos	• EP vehicle to Mars base
Mars Surface									•Phobos & Deimos	• Base to remote surface sys.

Not practical

High leverage

Beam Power EOTV Simulation

- Generates ground track over rotating Earth.
- Determines visibility and range from selected ground stations, up to 20 stations. Minimum beam elevation angle is a parameter.
- Calculates power transfer based on range, wavelength, apertures, available power and assumed beam quality factor.
- Numerically integrates orbit raising by thrust based on available power, input mass, and Isp.
- Current orbit state feeds back to above steps for every integration step.

Power Beaming: Key Issues and Questions

Near Term Applications

- Currently an Earth based laser transmission system coupled with an EOTV and or Lunar base, show the most promise for economic return.
- How does the performance (trip time and payload) of a power beam EOTV in an inclined orbit vary with number and distribution of ground stations?
- Assuming that power transmission to the Moon gets first priority, and considering typical weather and laser plant reliability, what is the beam power availability for the EOTV and how much is it expected to vary?
- How does the life cycle cost of a lunar surface/EOTV power beaming system trade with the conventional approach of cryogenic propulsion and nuclear reactors power for the lunar surface.

Beam Power Task Logic Flow

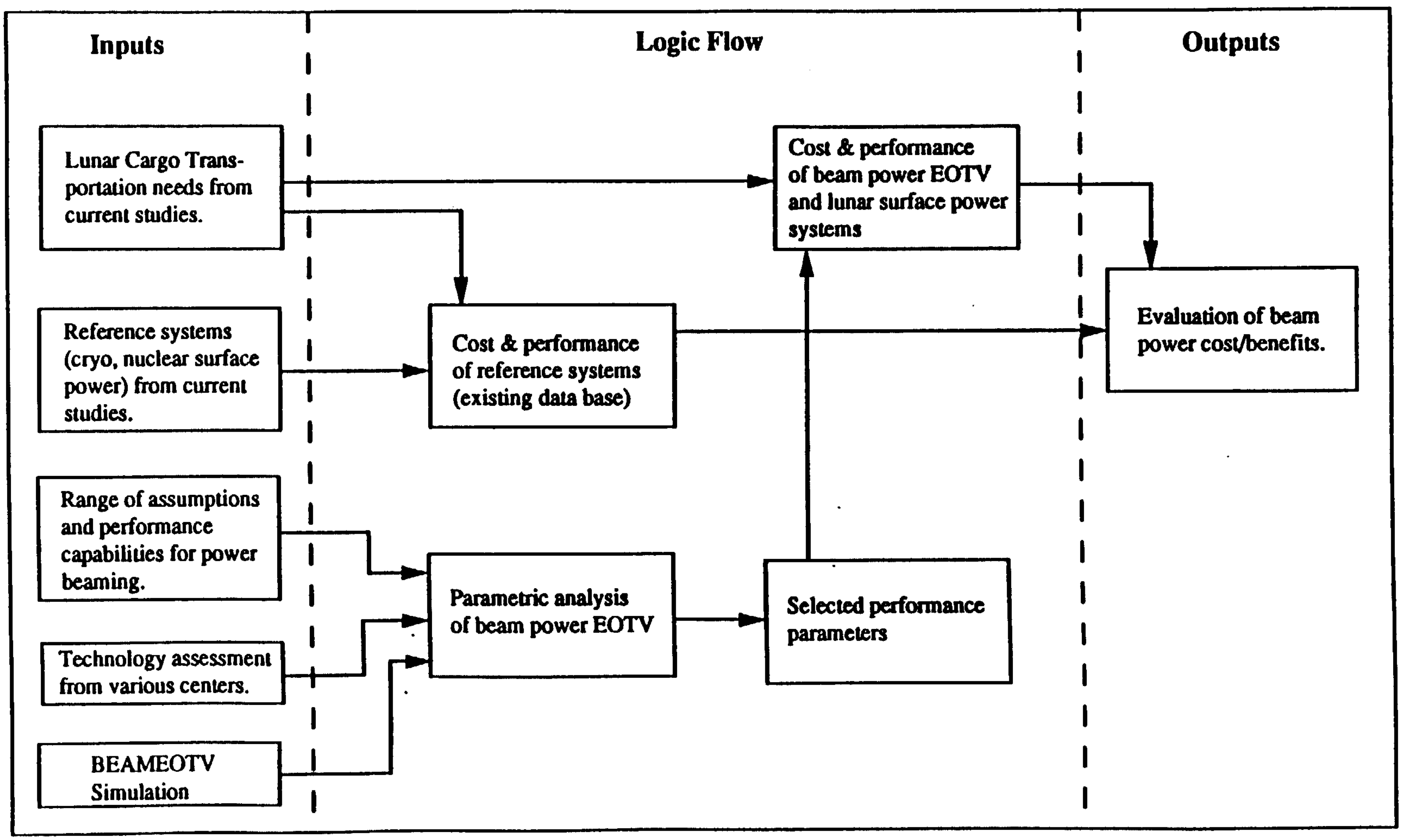

APPENDIX B

Minimum-Sized Lunar Campsite Analysis

Minimum-Sized Lunar Campsite Analysis

BOEING

February 21, 1991

Baseline Campsite Assumptions

- Crew of Four
- Mission Duration: 30 days
- Crew Vehicle Payload Capacity: 2-4 mt
- Storm Shelter Provided
- Open Loop ECLSS
- Open Cycle Fuel Cells
- External Systems (TCS, Power, C&T) are self-deployable
- Crew Return Vehicle provides extra level of redundancy

Baseline Campsite Summary

Systems	Mass (kg)	Volume (m^3)	Power (kWe)		Source/Comments
			Cont	Non-CAvg.	
Structures	5,933	106 Module * 7 Airlock	--	0.3	* Total volume which contains internal component volumes
Crew Systems	2,625	58	1.0	0.5	
ECLSS	1,070	5.1	2.2	0.2	Consumables mass not included
Internal EPS	495	0.75	0.4	--	
Internal TCS	405	1.5	0.03	0.5	
DMS/Communication	545	2.8	0.9	0.2	
IAV	50	0.75	--	0.3	
C&T	100	External	0.1	--	
External TCS	1,188	External	(2.2)	--	2.2 kWe during lunar day only
Power - Open cycle HW	360	External	--	--	Does not include fuel cell reactant mass (1955 kg)
- RFC pack	195	External	--	--	Deployment/Standby power
Science	1,565	8	0.65	1.0	
Storm Shelter	3,465	12	--	--	
15% Growth	1,945	13	--	--	Does not include science or storm shelter approach
Total	19,940	102	(7.5) 5.3	3.0	

Interior Configuration

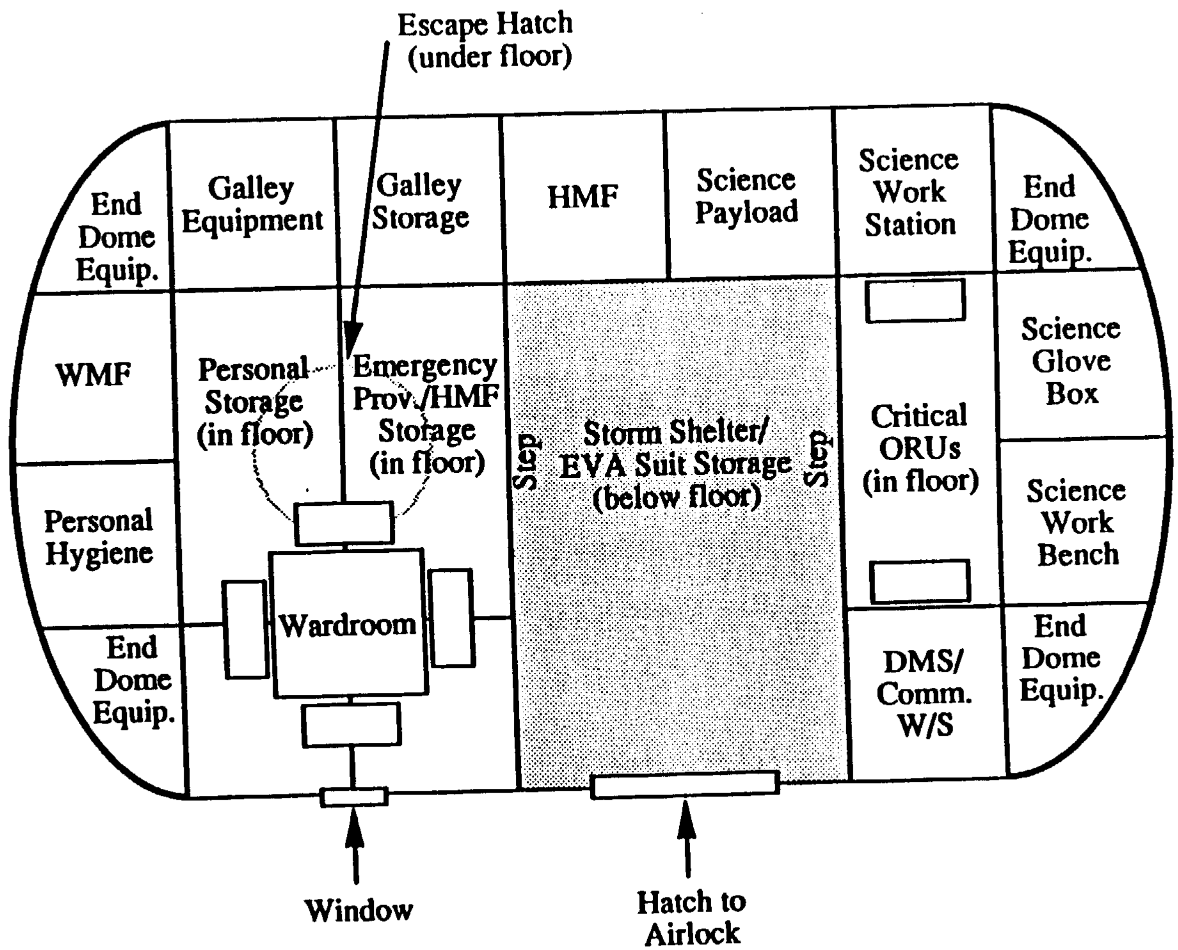

Floor Plan

Structure System Assumptions

- STCAEM Hab Trade structure system
- Subsystem structure mass includes components which vary with module length (e.g., ducting, plumbing, etc.)
- Airlock derived from SSF crewlock
- Barrel section length varies by rack equivalent widths (1.1m)
- Meteoroid/debris shield not required

Structure System Summary

System	Mass (kg)	Source/Comments
2 end domes	325	STCAEM Hab Trade/Aluminum (includes MLI)
2 hatch assemblies	844	Space Station Freedom/Aluminum
2 adapter bulkheads	207	Space Station Freedom/Aluminum
2 reinforcing rings	300	Space Station Freedom/Aluminum
External stairs	100	Boeing Study/Aluminum
Airlock	1,290	Space Station Freedom/Aluminum
Monocoque barrel	104 kg/m	STCAEM Hab Trade/Aluminum (includes MLI)
Internal Structure	225 kg/m	STCAEM Hab Trade/Aluminum (10% A&I, 5% Secondary)
Mechanisms	40	SSF SE21 (7/15/90) - Mass Properties
• ECLSS plumbing	24 kg/m	SSF SE21 (7/15/90) - Mass Properties
• DMS lines	30 kg/m	SSF SE21 (7/15/90) - Mass Properties
• EPS lines	51 kg/m	SSF SE21 (7/15/90) - Mass Properties
• IAV lines	3 kg/m	SSF SE21 (7/15/90) - Mass Properties
• TCS lines	77 kg/m	SSF SE21 (7/15/90) - Mass Properties

<u>Structure Formula Based on Volume</u>:
$\Sigma M = 3{,}106 + [514 \times (\text{barrel length in meters})]$

<u>Volume Data:</u>
Σ Endcone $V = 22.3\ m^3$
Σ Barrel $V/m = 15.2\ m^3/m$

Crew Systems Assumptions

- Minimal privacy provisions - STS precedent
  - e.g. deployable sleep bunks
- Crew Health Care equivalent to SSF PMC
  - SSF EMCC may be optimum
- <u>Absolute minimum</u> free volume requirements observed
  - 20% uncertainty factor included

Crew Systems Summary

Crew Systems	Mass (kg)	Volume (m^3)	Power (kWe) Cont	Power (kWe) Non-C Avg.	Source/Comments
Bunks	40	2.40*	--	0.05	Boeing study (12/12/88)
Personal Storage	100	2.00	--	--	Space Station Freedom
Crew Health Care	825	3.00	0.17	0.05	SSF PMC
Table and Chairs	35	1.00*	--	--	Boeing study (12/12/88)
Personal Hygiene/Waste Management	225	1.60	--	0.03	Space Shuttle
Galley/Storage	360	3.00	--	0.05	Space Shuttle Galley SSF Food Storage Rack
EVA Suite Maintenance	500	6.90	0.7	0.20	Space Station Freedom
External EVA Equipment	15	--	--	--	Space Station Freedom
Lights	50	--	0.1	0.05	STCAEM Lunar Module Study
Tools	25	Gen. Sto.	--	--	STCAEM Lunar Module Study
Critical CRUs/Gen. Sto.	350	2.00	--	--	Space Station Freedom
Emergency Provisions	100	0.50	--	0.02	Space Station Freedom
Free Volume	--	35.33**	--	--	Living Aloft by Mary Connors (NASA/Ames)
TOTAL	2,625	57.73	0.97	0.45	

*Stowed volume only

**Includes 20% uncertainty factor

ECLSS Assumptions

- Open loop
- Consumables (food, water, oxygen) delivered with crew
- No dedicated Avionics Air System
- Portable fire extinguishers
- No refrigerators or freezers
- Dual string carbon dioxide removal assembly (mole sieve)
- Dual string cabin air cooling system
- Single string Atmosphere Composition Monitoring Assembly
- Single string Trace Contaminant Control system
- Open loop water system includes distribution hardware
- Internal pressure - 14.7 psia

ECLSS Summary

ECLSS Subsystems	Mass (kg)	Volume (m^3)	Power (kWe)		Source/Comments
			Cont	Non-C Avg.	
THC (Structures)	360 (17.4)	2.0	.84	--	POWER: SSF/SE19 Electrical Power and Energy Reports (D683-10238-20)
FDS (Structures)	24 (21)	0.05	--	--	VOLUME: SSF Rack Alloc.
ACS (Structures)	60 (12)	0.05	.01	0.05	MASS: SSF/SE21 Mass Properties Report D683-10275-6
ARS (Structures)	525 (1.1)	2.0	1.35	--	
WRM (Structures)	100 (18)	1.0	--	0.1	
TOTAL	1,070 (23.6)	5.1	2.2	0.15	

Internal Systems Assumptions

- Includes Thermal Control System (TCS), Internal Audio/Video (IAV), Data Management System (DMS), and Electrical Power System (EPS)

- Systems in standoffs included in Structures mass and power values:
  - Each system summed for 4 SSF standoffs and divided by SSF module length (11 racks * 1.1m) to find mass per meter length

- Systems in enddomes/hatchways included here:
  - Each system summed for SSF endcones (EPS & TCS scaled for campsite application)
  - SPDA/TPDA modules (2 per powered rack) charged to each appropriate rack

- Internal TCS pump package, heat exchanger, and plumbing serve both systems and payloads

- Each "rack-based" function (Internal TCS pump, DMS W/S, Science, etc.) includes necessary system components internal to the rack, except:
  - No avionics air
  - Rack structure accounted for by Structures
  - ECLSS (including FDS) accounted for by ECLSS

- DMS/Comm Workstation based on SSF Element Control Workstation (ECWS)

Internal Systems Summary

Internal Systems (except ECLSS)	Mass (kg)	Volume ** (m^3)	Power (kWe)		Source*/Comments
			Cont	Non-C Avg.	
EPS					
Exo-rack (minus standoff)	495.0	0.75	0.4		1/2 of SSF SPDA & DDCU Numbers
DMS					
Exo-rack (minus standoff)	173.6	0.75	0.36		
DMS/Comm W/S	372.4	2.0	0.55	0.22	Based on SSF ECWS
DMS Subtotal	546.0	2.75	0.91	0.22	
IAV					
Exo-rack (minus standoff)	46.6	0.75		0.26	
TCS					
Exo-rack (minus standoff)	328.4	0.75	--	--	1/2 of SSF Central Thermal Bus Numbers
Pump package/HX	76.1	0.7	0.03	0.52	
Int. TCS Subtotal	404.5	1.45	0.03	0.52	

*SSF WP01 SE19 (4/15/90)
SSF WP01 SE21 (7/15/90)
Level II Power Allocation Report and Margin Analysis, Rev. A SHQ-321-0008A, Nov. 1, 1990

**Total Exo-rack (minus standoff) volume assumed ~ 3.0 m^3 (0.75 m^3 for each system)

External Systems Assumptions

- Includes TCS and Communications & Tracking (C&T)

- External TCS

  - Baseline includes single loop heat pump for external TCS
  - Radiator size doubled to account for worst sun angle case
  - Daylight Power = 14.3 kW
  - TCS heat pump requires 2.2 kW during the lunar day only
  - Shield mass accounts for deployable system

- C&T system based on Lunar Rover work

External Systems Summary

External Subsystems (except Power)	Mass (kg)	Volume (m^3)	Power (kWe) Cont	Power (kWe) Non-C Avg.	Source/Comments
C&T					
Antennas, lines, etc.	20		0.10	--	
Deployable structure	80		--	--	
C&T Subtotal	100		0.10		From lunar rover estimates
TCS					
Transport loop	206		2.2	--	
Radiator	329		--	--	
Shield	653		--	--	
Ext. TCS Subtotal	1188		2.2		Daylight power only

Power System Assumptions

- Lunar day length - 335 hrs.
- Lunar night length - 375 hrs. (baseline), 145 hrs. (20 day mission)
- Open cycle fuel cell reactants are cryogenic
- Solar arrays provide power for daytime power needs
- Fuel cells provide power during lunar night
- Peak power loading is the sum of continuous power plus the power required for other components that may be turned on at the same time (14.3 kW during the lunar day and 12.1 kW during the lunar night)
- Average power is the sum of continuous power plus the product of non-continuous power and duty cycle (10.5 kW during the lunar day and 8.3 kW during the lunar night)
- Solar arrays are sized for peak power loading
- Fuel cell reactants are sized for average power
- 0.5 kW regenerative fuel cell pack provided for initial subsystem deployment and standby operations for vacant campsite.

Power System Summary

Power System Components	Open Cycle		RFC Pack
	Baseline	20 day	
Solar Array	158	158	0
Fuel Cell System			
Hardware	203	203	20
Reactants & Tankage	1955 *	762 *	175 **
TOTAL - Campsite	361	361	195
- Resupply	1955	762	0

* Open cycle tank fraction is 0.42 kg tank/kg reactant for cryogenic storage
** RFC tank fraction is 1.1 kg tank/kg reactant for high pressure storage

Internal Science Assumptions

- A representative set of internal science equipment selected
- Workstation
  - External science monitoring
  - Data reduction
  - Telerobot management
- Science glovebox
  - Isolated experiments
  - Sample evaluation
- Science workbench
  - Open work area
  - Diagnostics
  - Power tools
- Science payload is interchangeable
- Locating science glovebox adjacent to workbench may allow combination into Maintenance Workstation (MWS)

Internal Science Summary

Internal Science	Mass (kg)	Volume (m^3)	Power (kWe)		Source*/Comments
			Cont	Non-C Avg.	
Workstation	372.4	2.0	0.55	0.22	Based on SSF ECWS
Glovebox	410.0	2.0	0.03	0.14	Based on SSF Materials Processing Glovebox
Workbench	381.1	2.0	0.03	0.39	Based on SSF Life Sciences Workbench
Payload	400.2	2.0	0.07	0.23	Based on generic 3 kW SSF payload rack
Science Subtotal	1563.7	8.0	0.68	0.98	

*SSF WP01 SE19 (4/15/90)
SSF WP01 SE21 (7/15/90)
Level II Power Allocation Report and Margin Analysis, Rev. A SHQ-321-0008A, Nov. 1, 1990

Storm Shelter Assumptions

- Assumed acceptable dosage of 25 rem
- Storm shelter supplies included as part of emergency provisions (see Crew Systems)
- Power, C&T, DMS, etc. are accessed within storm shelter via normally functioning equipment
- Storm shelter located under floor near middle of module:
  - Protection required based on 1972 solar flare event
  - Lunar surface effectively reduces radiation flux by 50%
  - Water couches provide 30° of protection along each module wall
  - Lower 120° protected by lunar surface
  - Campsite components provide at least one fourth of required shielding
  - Additional water protection added above and along internal sides of shelter
- Fuel cell reactant mass is not credited to storm shelter shielding
- Water produced by open cycle fuel cells may be cycled to storm shelter storage tanks to maintain/improve protection levels
- ECLSS use of storm shelter water in exchange for brine, contaminated water, etc. may be feasible for reducing consumable resupply
- Detailed analysis required to verify and refine shelter estimates

Storm Shelter

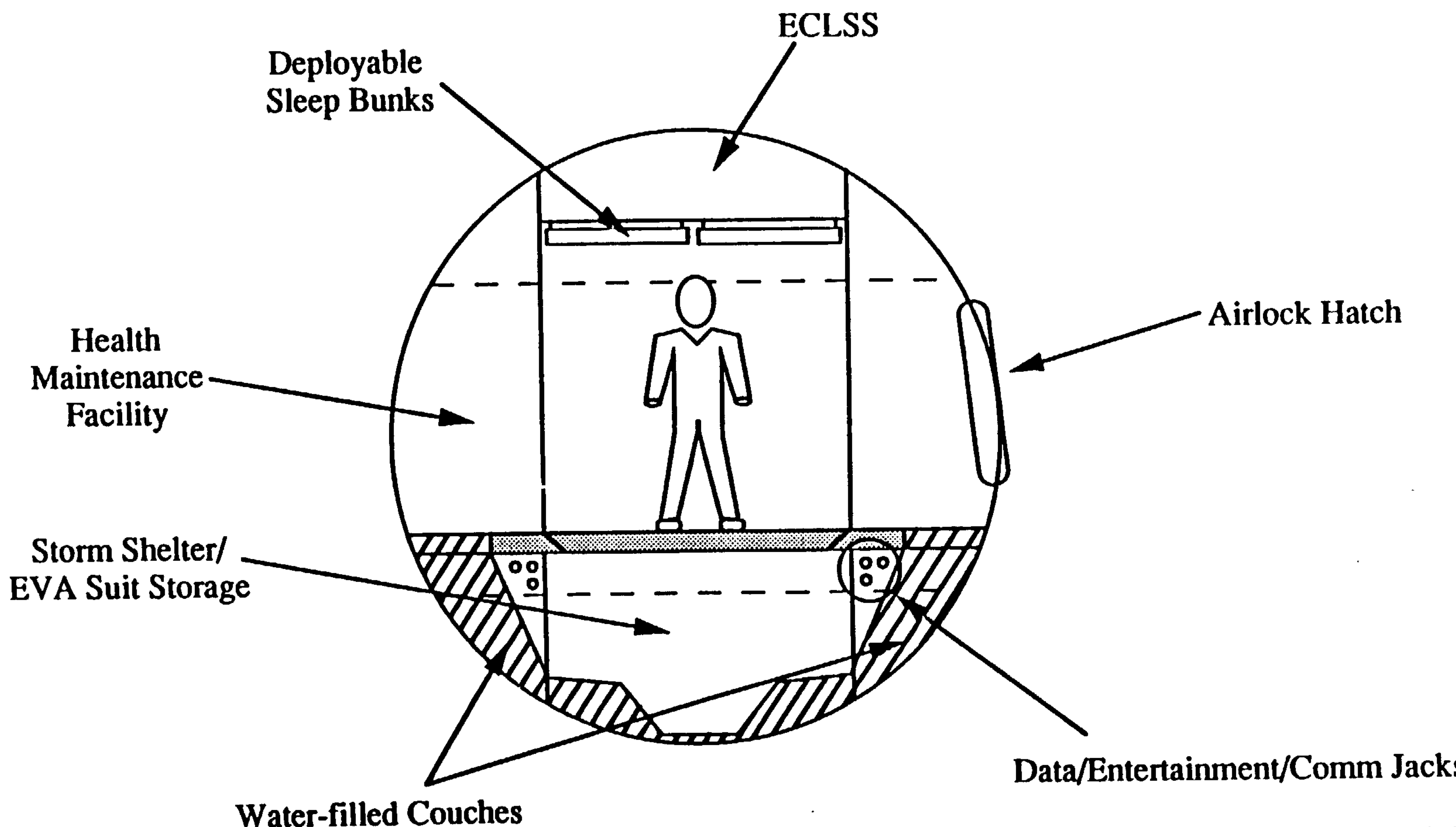

(Emergency Supplies include food, drink, books, P-MPAC for statusing/monitoring, communication headsets, medical/dental supplies, minor surgical instruments, flashlights,etc.)

Cross Section

Storm Shelter Summary

Baseline Storm Shelter	Mass (kg)	Volume (m^3)	Power (kWe)		Source/Comments
			Cont	Non-C Avg.	
Water Couches	734				Provides 30° of coverage along each module wall *
Structure	500				Assumed equivalent to 5+ SSF racks
Additional Shielding	2230				Supplements top and internal sides protection
Shelter Subtotal	3464	12.0	--	--	Highly sensitive to vehicle configuration

* Lower 120° assumed to be protected by lunar surface

NASA/MSFC Mass Reduction Options

OPTIONS	Option Reductions			Subsystem Mass Impacts		ΣΔM	Impact on Power System Resupply
	Mass (kg)	Volume[1] (m^3)	Pwr Avg (kWe)	Power	TCS		
No Science	1565	8.0	(1.63)	- 29	- 68	- 1662	-384 kg reactants (baseline) -150 kg reactants (20 days)
MTC/SSF Medical	610	2.5	(0.18)	- 4	- 10	- 624	-42 kg reactants (baseline) -16 kg reactants (20 days)
or							
STS First Aid	817	2.97	(0.22)	- 5	- 12	- 834	-52 kg reactants (baseline) -20 kg reactants (20 days)
Reduce Crew to 3	190	12.0	(0.2)	- 6	- 14	- 210	-47 kg reactants (baseline) -18 kg reactants (20 days)
Composite Structure Material (106 m^3)	714[2]	--	--	--	--	- 714	
Reduce Staytime to 20 days	--	--	--	0	--	0	-1193 kg reactants to be delivered with crew; no impact on campsite
Maximum reduction (all options)						3676 kg	

(1) Total volume reduction must be more than 16.75 m^3 to reduce module length by 1 rack equivalent (1.1 m) which reduces aluminum module mass by 565 kg (composite module reduction is 256 kg).
(2) Use of composites greatly increases DDT&E costs

Composite Materials Mass Savings Potential

System	Mass (kg)	Potential Savings (%)	Potential Savings (kg)	Source/Comments
2 end domes	325	15	49	Use SiC/Al filament wound composite instead of welded Al.
2 hatch assemblies	844	12	101	Use discontinuous SiC reinforced Al instead of monolithic Al structure.
2 adapter bulkheads	207	12	25	Use discontinuous SiC reinforced Al instead of monolithic Al structure.
2 reinforcing rings	300	12	36	Use discontinuous SiC reinforced A1 rolled extrusions instead of Al.
External stairs	100	50	50	Use graphite reinforced epoxy or polymide composites instead of Al.
Airlock	1,290	10	129	(same as comments for hatch assemblies and Monocoque barrel)
Monocoque barrel	572	15	86	Use SiC/Al filament wound composite instead of welded Al.
Internal structure	1,238	15	186	Use graphite reinforced epoxy or polymide composites instead of Al.
Mechanisms	40	10	4	Use Be and Ti in lieu of Al and steels.
• ECLSS plumbing	132	5	7	Use plastics and Al instead of steel. Consider metal coatings.
• DMS lines	165	10	17	Develop graphite composite electronic enclosures. Incorporate high temperature superconductors and GaAs semiconductors.
• EPS lines	281	10	3	
• IAV lines	17	0	--	SOTA fiber optics
• TCS lines	424	5	21	Improved thermal insulation, graphite heat conductors, & Be structure.
TOTAL	5,933	12	714	See Notes

Notes:
1. Potential mass savings were estimated on the basis of specific strength and stiffness factors for stress limited and deflection limited designs.
2. Potential mass savings reflect technical feasibility without regard to development risks.
3. Trade studies must be conducted to justify implementation.

ADVANCED CIVIL SPACE SYSTEMS

Increased Cost of Advanced Materials

BOEING

Estimated Costs vs. Potential Mass Savings

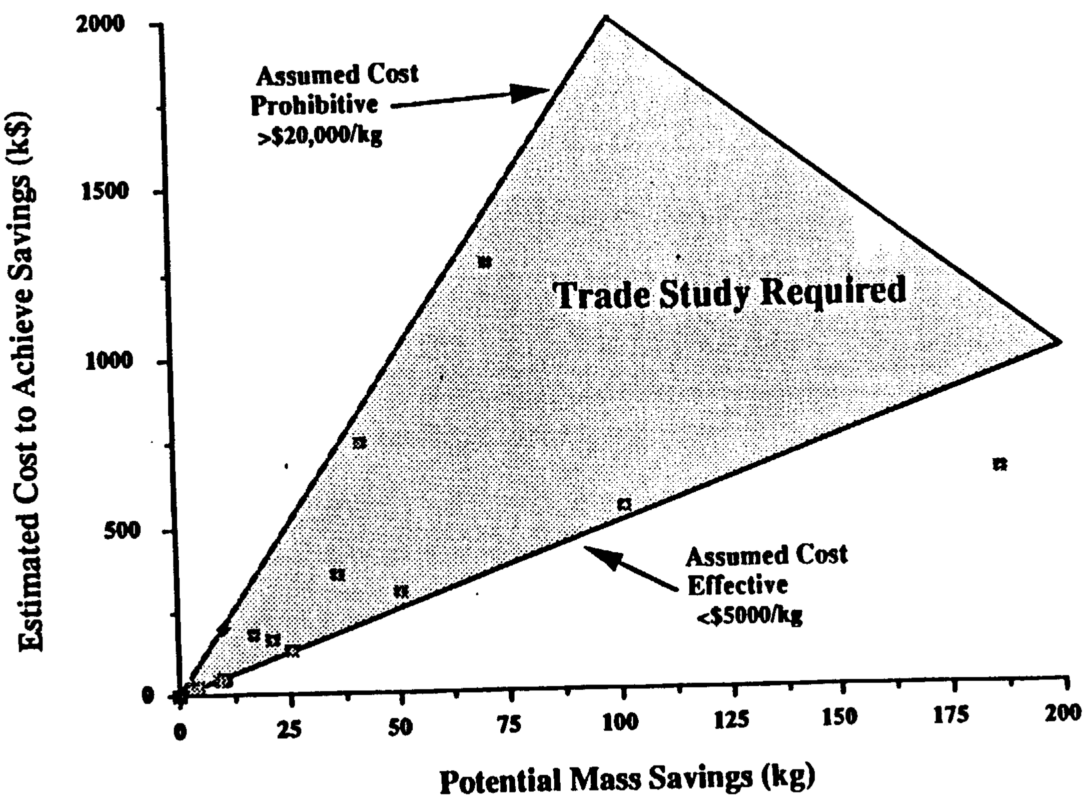

- Estimated from past comparable material development costs

Delivered With Crew Vehicle

- Crew related
  - Gear
  - EMUs
  - In-Transit Life Support

- Campsite resupply

Description	Baseline	20-Day
Life Support Resources	Consumables * 1,066 Expendables 70	710 47
Power System Reactants	1955	762
Rover @ 520 kg	TBD	TBD
Science Equipment	TBD	TBD
EVA Gases (one/day)	211	141
Repress Gases	TBD	TBD

* Open cycle fuel cell water production and exchange with storm shelter water may be used to reduce/eliminate water resupply.

Remaining Issues

- Storm Shelter calculation uncertainties
- Selection of science complement
- Logistics of resupplying fuel cell reactants
- Standby operation between non-contiguous visits
- Details for self-deploying and self-activating systems
- EMU servicing and maintenance
- External science and service/maintenance requirements (e.g. rover battery recharge)

Minimum-sized Campsite Summary

- Minimum campsite able to provide significant capabilities beyond Apollo is approximately 20 mt

- Reasonable confidence in campsite weights
  - SSF PDR data used for majority of campsite components
  - Relatively detailed component analysis
  - 15% growth margin applied

- Minimizing campsite mass drives selection of open loop ECLSS and open cycle fuel cells

- Regenerative life support and fuel cells would reduce resupply mass for long duration and/or multiple campsite missions

- NASA policy decisions will determine science, medical, and storm shelter requirements

- Optimization of campsite and crew delivery flights are interdependent